

OPTICAL MODEL ANALYSIS OF $O^{16}(\alpha,\alpha)O^{16}$ AT 65 MEV

A thesis
submitted to the
Faculty of Graduate Studies
University of Manitoba
in partial fulfillment of the
requirements of the degree of
Master of Science

by

David Yang-man Tseng

Department of Physics
The University of Manitoba
Winnipeg, Manitoba

December, 1967



TABLE OF CONTENTS

List of Figures	i
Acknowledgments	ii
Abstract	iii
Chapter I - 1-1 Introduction	1
1-2 Physical Aspect of the Optical Model	5
1-3 The Phenomenological Optical Potential	9
Chapter II The Optical Model Analysis of $O^{16}(\alpha, \alpha)O^{16}$	15
2-1 Theory of Optical Model Elastic Scattering and Programming	15
2-2 Automatic Search Routine	27
Chapter III Optical Model Potentials and Parameter Ambiguity	34
3-1 $\alpha-O^{16}$ Optical Model Potentials	34
3-2 Optical Parameter Ambiguities	51
3-2.1 Vr_0^n Ambiguity	52
3-2.2 Potential Depth Ambiguity	57
3-3 The Surface Region of $\alpha-O^{16}$ Optical Potentials	59
3-4 Summary and Conclusion	59
Appendix Automatic Search and Elastic Scattering Programs	63
References	72

LIST OF FIGURES

1.	Real Part of Optical Potential	13
2.	Imaginary Part of Optical Potential	14
3.	Three-Parameter Unstable Search	30
4.	Four-Parameter Convergent Search	33
5.	Fitting Using Volume Absorption	36
6.	Fitting (V=305.2 Mev)	37
7.	Fitting (V=288.0 Mev)	38
8.	Fitting (V=275.2 Mev)	39
9.	Fitting (V=256.9 Mev)	40
10.	Fitting (V=249.1 Mev)	41
11.	Fitting (V=198.3 Mev)	42
12.	Fitting (V=172.6 Mev)	43
13.	Fitting (V=135.8 Mev)	44
14.	A) Modulus of Scattering Coefficient	47
	B) Phase of Scattering Coefficient	48
15.	Amplitude of the Radial Wavefunction (V=305.2)	49
16.	Amplitude of the Radial Wavefunction (V=198.3)	50
17.	$ R_0 $ for Group I Potentials	54
18.	$ R_0 $ for Group II Potentials	55
19.	$ R_0 $ for the Potentials 3, 8, and 9	56
20.	Variation of $\frac{d\sigma}{d\Omega}$ with r_c	62

ACKNOWLEDGMENTS

To my supervisor, Dr. B. Hird, my grateful thanks for his suggestion of the problem and for his patient guidance and constant encouragement throughout the course of this work.

To Dr. T. Y. Li my sincere thanks for his assistance and many important discussions.

My thanks are also due to Mr. C. Kost for discussions concerning the experimental aspect of this work, and to Mr. M. K. Liou for suggesting the Feynman diagrams.

The financial assistance from the University is gratefully acknowledged

ABSTRACT

The angular distributions of the scattering of alpha particles at 65 Mev have been fitted using Saxon-Woods and derivative Saxon-Woods form factors for the real and imaginary parts of the optical potential respectively. The analysis yielded a series of potentials. The lack of uniqueness was due to two types of parameter-ambiguity. The first type was that the optical parameters were allowed to vary, with the quantity Vr_0^2 kept constant. It was found that the potentials of this type generated same number of half-waves inside the nucleus. The second type was that the parameters could be adjusted so that they produce one or more integral multiple half-waves inside the nucleus such that the corresponding wavefunctions far away from the nuclear field were the same.

This analysis defined the optical potential for the alpha particles fairly well near the surface.

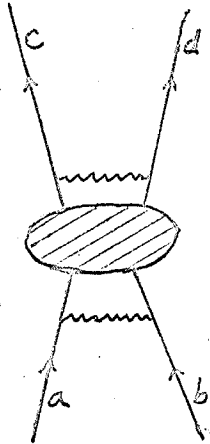
CHAPTER I

1-1 INTRODUCTION

There is a current interest in applying the distorted-wave-Born-approximation (DWBA) method to analyzing nuclear reactions. However, the distorting potentials in the entrance and/or exit channels must be known. These are represented by the saw-toothed lines in Diag. 1. a and b are the particles in the entrance channel, and c and d, the particles in the exit channel. They may be in the excited states. It is difficult, in the pioneering days of searching the nuclear forces, to obtain the exact interacting potentials which may consist of the central, spin-orbit, exchange, and tensor components. The many-body effects come into play if the interaction involves complex particles rather than single nucleons. Fortunately, a phenomenological two-body optical model potential can be found by analyzing the experimental elastic scattering data for the relevant particles at the required energies. Such a potential will describe the averaged behaviour of the interacting particles. This is the initial stimulus of the thesis. Since it is impossible at present to prepare a target in a definite excited state, the optical model potential obtainable are only between

(2)

ground states.



Diag. 1.

The detailed analyses of $O^{16}(\alpha, \alpha)O^{16}$ at 65 MeV⁷⁾ will be presented in Chapter 2. The results can be used in the reaction, say $O^{16}(\alpha, p)F^{19}$ (8).

The initial work of the optical model was due to Fernbach, Serber, and Taylor¹⁾, and later, was developed by LeLevier and Saxon²⁾ in 1952, and Feshbach, Porter, and Weisskopf²⁾ in 1954 by the important stimulation of Barschall's slow-neutron experiments.

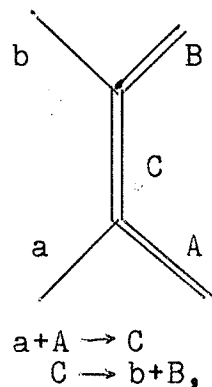
The simplest potential describing the nucleon-nucleus inter-

(3)

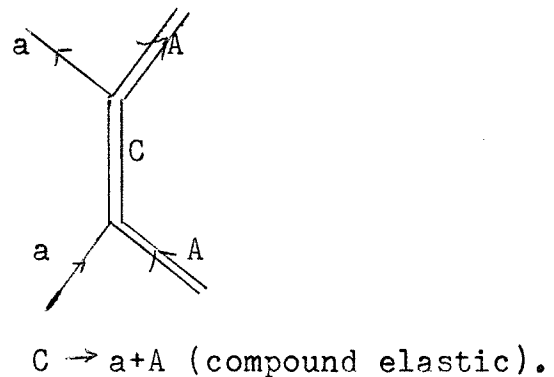
action was Bethe's real well potential,

$$V_n(r) = \begin{cases} -V_0, & r \leq R \\ 0, & r > R \end{cases}$$

This simple model was unable to interpret the experimental results at low energies, such as large capture cross-sections, sharp resonance spacings, and the sensitiveness of the cross-sections to energy. It is because, at low energies (< 10 Mev), the many-body effect is predominant. Bohr's compound nucleus model successfully described these phenomena. This model considers the nuclear reactions in two steps. In the first step, the target nucleus absorbs the incident particle to form a compound nucleus state which lives a relatively longer life than the nucleon transit time. In the second step, the compound nucleus decays. The processes are described by the following diagrams.



or



The compound elastic scattering might occur. This is experimentally indistinguishable from the shape elastic scattering. Only shape elastic scattering will be considered throughout the thesis.

At energies above about 10 Mev, the compound nucleus effects are greatly reduced. Fernbach et al¹⁾ thus proposed a complex potential model. Their initial idea was that the nucleon-nucleus elastic scattering could be approached by the scattering of a wave by a refracting and absorbing sphere. It is well-known in optics that the process can be described by means of a complex index of refraction. The imaginary part accounts for the absorption. They used WKB approximation and related the imaginary part to the mean free path of the incident nucleon inside the target nucleus. This enabled them to reproduce the angular distributions for the small-angle scattering.

1-2 PHYSICAL ASPECT OF OPTICAL MODEL

The optical model potential may be defined as the complex potential which represents the energy-averaged behaviour of the nuclear system in the direct interaction process. The possibility of taking the average is limited by the energy of the incident particles, i.e., the resonance energy E_s is larger than the spacings Γ between levels. From the experimental point of view, the optical model description is satisfactory when the resolving power of the detector is low, and when the energy width of the incident beam is larger than the individual level spacings. Therefore the optical model is applicable for energies of about 10 Mev in light nuclei, in which the level spacing is of the order of $\Gamma \simeq 0.1\text{--}0.5$ Mev for incident energy $E < 5$ Mev. The optical model is more successful when it is applied to heavy nuclei, even when the energy of the incident particle is lowered to a few KeV⁴⁾.

Now we apply the above idea to the average cross-sections. The energy-average of a quantity $f(E)$ is defined by

$$\bar{f} = \frac{1}{\Delta E} \int_{\Delta E} f(E') dE', \quad (1-1)$$

where ΔE includes many individual resonance levels.

(6)

The scattering amplitude for spinless particles is

$$f = \frac{1}{2k} \sum (2\ell+1)(1-\eta_\ell)P_\ell(\cos\theta). \quad (1-2)$$

When only short range forces are considered so that the Coulomb force is neglected the sum has a finite number of terms. The scattering matrix elements η_ℓ are related to the phase shifts δ_ℓ by

$$\eta_\ell = e^{2i\delta_\ell}. \quad (1-3)$$

The elastic scattering cross-section is then given by

$$\sigma_{\text{elastic}} = \frac{\pi}{k^2} \sum_{\ell} (2\ell+1) |1-\eta_\ell|^2. \quad (1-4)$$

The energy-average of σ is

$$\begin{aligned} \bar{\sigma}_{\text{elastic}} &= \frac{\pi}{k^2} \sum (2\ell+1) \frac{1}{\Delta E} \int_{\Delta E} |1-\eta_\ell|^2 dE \\ &= \frac{\pi}{k^2} \sum (2\ell+1) \overline{|1-\eta_\ell|^2} \\ &= \frac{\pi}{k^2} \sum (2\ell+1) \left[|1-\bar{\eta}_\ell|^2 + |\bar{\eta}_\ell - \eta_\ell|^2 \right] \end{aligned} \quad (1-5)$$

$\bar{\eta}_\ell$ is obtained from the optical model calculation. The first term in Eq.(1-5) represents the optical elastic

(7)

scattering. $\overline{|\eta_\ell - \bar{\eta}_\ell|^2} = \overline{|\eta_\ell|^2} - |\bar{\eta}_\ell|^2$ is the mean-square fluctuation of η_ℓ about its average. We thus define

$$\sigma_{fl}^{(\ell)} = \frac{\pi}{k^2} (2\ell + 1) \overline{|\eta_\ell - \bar{\eta}_\ell|^2} \quad (1-6)$$

as the fluctuation cross-sections.

Carrying out the energy-average for the reaction cross-section, we obtain

$$\begin{aligned} \bar{\sigma}_r &= \frac{\pi}{k^2} \sum_{\ell} (2\ell + 1) \left(1 - \overline{|\eta_\ell|^2} \right) \\ &= \frac{\pi}{k^2} \sum_{\ell} (2\ell + 1) \left[(1 - |\bar{\eta}_\ell|^2) - \overline{|\eta_\ell - \bar{\eta}_\ell|^2} \right]. \end{aligned} \quad (1-7)$$

The quantity

$$\sigma_{\text{absorption}} = \frac{\pi}{k^2} \sum_{\ell} (2\ell + 1) (1 - |\bar{\eta}_\ell|^2)$$

is the optical model absorption cross-section.

Eq.(1-5) and (1-7) can be written

$$\bar{\sigma}_{\text{elastic}} = \sigma_{\text{opt.}} + \sigma_{fl},$$

$$\bar{\sigma}_r = \sigma_{\text{absorption}} - \sigma_{fl}.$$

These suggest that σ_{fl} is due to compound elastic

(8)

scattering. At low energies it is possible to detect the fluctuations by means of a high resolving power detector. At higher energies the resonance levels crowd together, and only the averaged cross-section is observed. The fluctuation is reduced to negligible values.

The optical model can also be applied to high energy (<200 Mev) scattering such as nucleon-nucleus and pion-nucleus elastic scatterings. Special approximation method should be used. High energy nucleon-nucleus scattering, for instance, may be approached by Watson's two-body multiple scattering⁹⁾.

The detailed mathematical treatments concerning the foundations of the optical model were given in the review article by Feshbach (1958) and in the nuclear reaction theory by Humblet and Rosenfeld (1961).

1-3 THE PHENOMENOLOGICAL OPTICAL POTENTIAL

The forces between a nucleon (or a complex particle) and a nucleus are of the two types, Coulomb and nuclear.

$$V(\underline{r}) = V_c + V_n$$

The Coulomb potential is well known and can be calculated from the charge distribution of the target nucleus. In the following analyses of the elastic scattering between two magic nuclei $\alpha + O^{16}$, the charge of α -particle will be considered as a point charge, and the charge of oxygen nucleus is uniformly distributed throughout a sphere of radius R_c ,

$$V_c = \begin{cases} \frac{ZZ'e^2}{2R} \left(3 - \frac{r^2}{R^2}\right) & \text{for } r \leq R_c, \\ \frac{ZZ'e^2}{r} & \text{for } r > R_c. \end{cases} \quad (1-8)$$

We relate R_c to the atomic mass number A by

$$R_c = r_c A^{1/3}.$$

Nuclear forces are represented by the optical potential

$$V_n(r) = Uf(r) + iWg(r) + \left(\frac{\hbar}{\mu c}\right)^2 \left\{ U_{so} f_{so} + iW_{so} g_{so} \right\} \underline{\sigma} \cdot \underline{\ell} \quad (1-9)$$

(10)

For the α -particle scattering the spin-orbit term is omitted. Eq.(1-9) becomes

$$V_n(r) = Uf(r) + iWg(r), \quad (1-9)'$$

where U and W are constants or 'potential depths'. $f(r)$ and $g(r)$, which determine the form of the nuclear potential and are functions of several variable parameters, are called form factors of the optical potential. There is an ambiguity of choosing the form factors. At least ten different functions have been used by the previous authors⁵⁾. At medium high energies (<100 MeV) the form factors should satisfy the following standards so that its parameters will have physical meaning and be comparable with the nuclear data obtained from different experiments. Otherwise the phenomenological optical potential will become merely a parametrization of the experimental data⁶⁾. The real form factor $f(r)$ should characterize the following nuclear properties: (1) all the nuclear forces fall off exponentially at large distances; (2) inside the nucleus, owing to the short-range character of the nuclear forces, the net force on the incident particle is approximately zero. The Saxon-Woods form factor

$$f_{sw}(r) = \frac{1}{1 + \exp\left(\frac{r-R}{a}\right)} \quad (1-10)$$

meets the requirements. $f_{sw}(r)$ is nearly constant when $r < R$,

(11)

and falls off quickly at $r \simeq R$. For heavy nuclei, this corresponds approximately to the region where the density of the nuclear matter is falling rapidly. R is thus recognized as the nuclear radius, and related to the atomic mass number A in the usual way

$$R = r_0 A^{1/3}.$$

The radius parameter r_0 has been obtained from other sources of the nuclear data, $r_0 \simeq 1.3 - 1.7$ fermis.

The interaction is essentially surface for light nuclei. This is shown in the Fig. 1 and Fig. 2.

The function $f(r)$ falls sharply or gradually around $r=R$ according to the value of a is large or small. a is referred to as the surface diffuseness parameter or the thickness of the surface layer.

It is relatively difficult to choose a function for the form factor $g(r)$. The Saxon-Woods (volume absorption) and the derivative of the Saxon-Woods form factors have been used in the present analysis. Both of them give good fits to the experimental data according to the χ^2 standard. The derivative Saxon-Woods form seems more favorable, and gives better account for the third bump of the angular distribution at large angles. The normalized $g_{sw}(r)$ is

(12)

given by

$$g_{sw}(r) = \frac{4 \exp\left(\frac{r-R}{a}\right)}{\left(1 + \exp\left(\frac{r-R}{a}\right)\right)^2} \quad (1-11)$$

$g_{sw}(r)$ has a maximum at $r=R$ (Fig. 2). The physical basis of using this form factor for the imaginary part is that the incident particle interacts more strongly with the surface nucleons than with the nucleons inside the nucleus due to the Pauli exclusion principle. The imaginary part is thus not proportional to the nucleon density. Jones¹⁰⁾ has calculated the radial dependence of the imaginary part of the optical potential using Fermi-Thomas approximation which assumes that a Fermi energy can be defined as a function of nucleon density and hence of radial position r . The calculation revealed that the imaginary part of the optical potential was maximum at the nuclear surface. The effectiveness of the exclusion principle diminishes as the energy of the incident particle increases. The requirement that $g(r)$ should be surface peaked is removed.

(13)

Fig. 1

Real Part of Optical Potentials

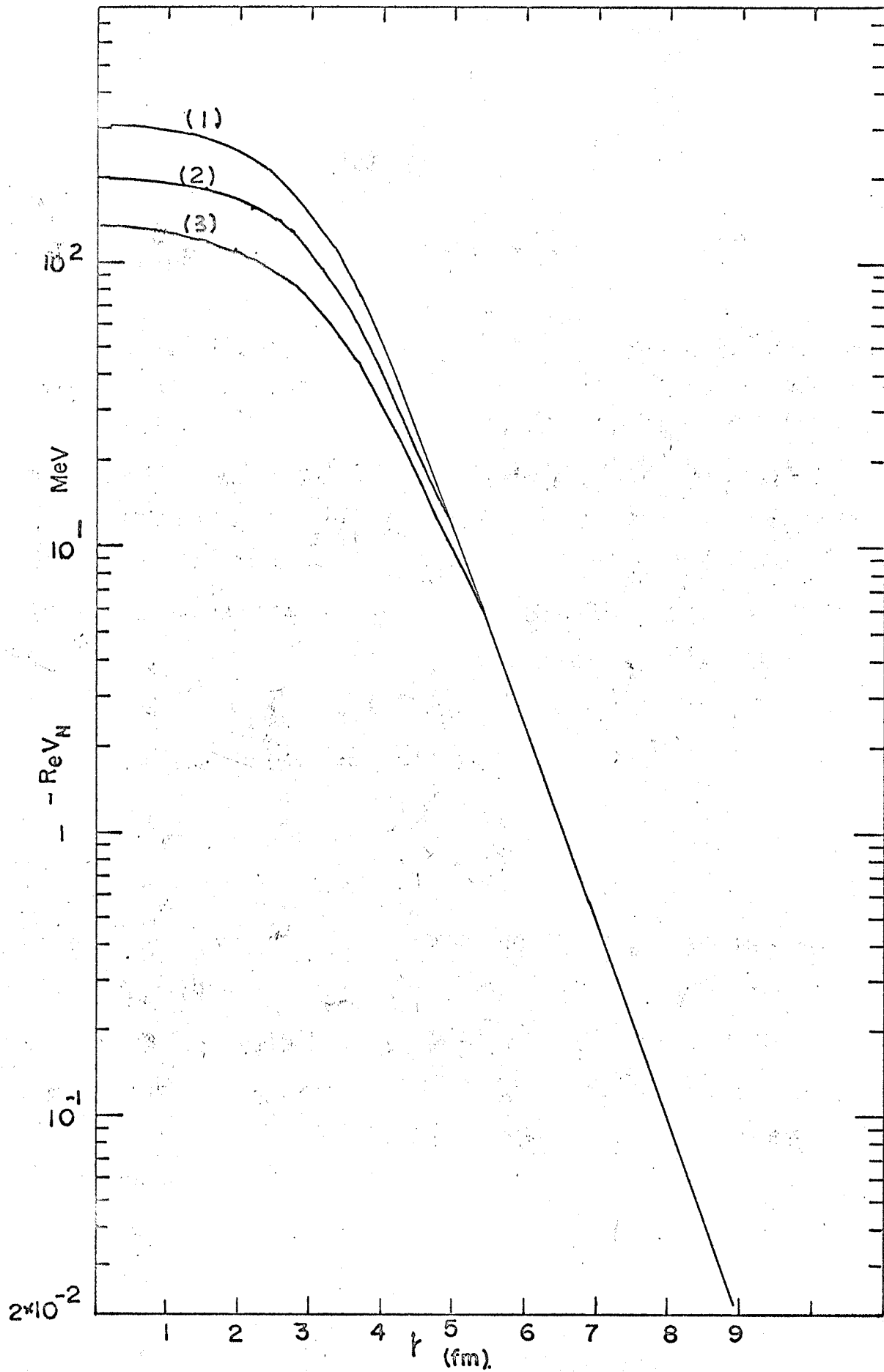


Fig. 1

Fig. 2

The imaginary part (surface absorption) of the optical potentials.

<u> </u>	<u>W_s (Mev)</u>
1	29.4
2	27.1
3	26.2
4	25.8
5	24.0
6	22.4

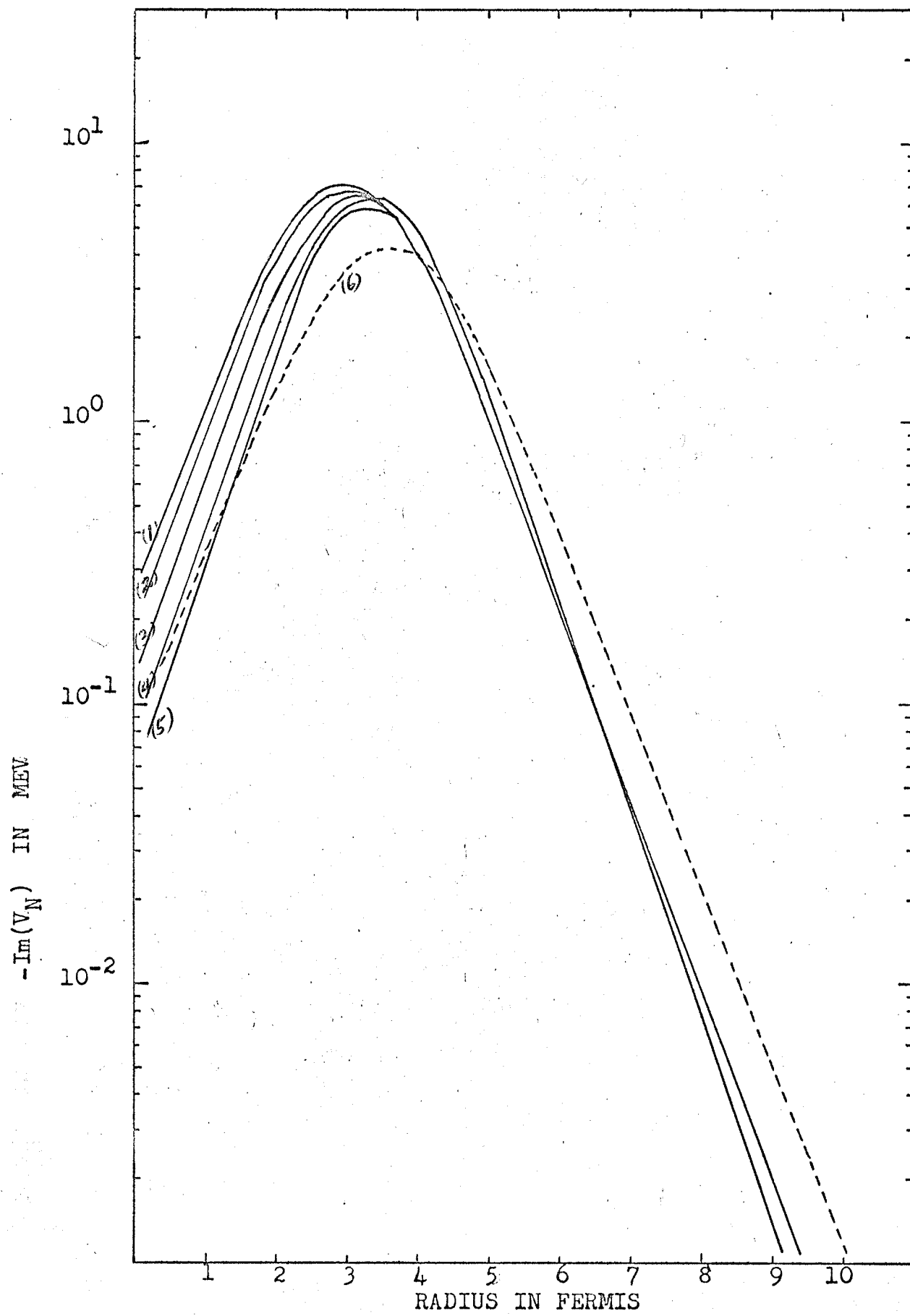


Fig. 2

CHAPTER IITHE OPTICAL MODEL ANALYSIS OF $O^{16}(\alpha, \alpha)O^{16}$

2-1 Theory of Optical Model Elastic Scattering and Programming

The differential cross-sections can be obtained by solving the Schroedinger equation if the interacting potential is given. However, the process is not reversible. One thing we can do is to optimize the parameters of the phenomenological optical potential which will give good fit to the experimental data. The quantity we choose to measure the goodness-of-fit is χ^2 which is a measure of the difference between the experimental and theoretical distributions.

$$\chi^2 = \sum_{i=1}^n \frac{(\mathcal{N}_T^i - \mathcal{N}_E^i)^2}{\mathcal{N}_T^i}$$

where \mathcal{N}_T^i and \mathcal{N}_E^i are the theoretical and experimental numbers of counts respectively for the i^{th} measurements. In the present case only differential cross-sections are considered. The number \mathcal{N}_E^i is proportional to the differential cross-section $\sigma_E(\theta_i)$ measured at the centre-of-mass angle θ_i . We have

$$\sigma_E(\theta) = c\mathcal{N}_E^i, \quad \sigma_T(\theta_i) = c\mathcal{N}_T^i, \quad \text{and} \quad \int \sigma_E(\theta_i) = c\sqrt{\mathcal{N}_E^i}$$

where $\delta\sigma_E$ is the standard deviation in statistics. The proportional constant c characterizing the absolute normalization has a deviation which can be derived from the above relations,

$$c = \frac{(\delta\sigma_E)^2}{\sigma_E}.$$

Then,

$$\chi^2 = \sum_i \left(\frac{\sigma_T(\theta_i) - \sigma_E(\theta_i)}{\delta\sigma_E(\theta_i)} \right)^2 \frac{\sigma_E(\theta_i)}{\sigma_T(\theta_i)}$$

$$\approx \sum_i \left(\frac{\sigma_T(\theta_i) - \sigma_E(\theta_i)}{\delta\sigma_E(\theta_i)} \right)^2,$$

where we have put $\sigma_T \approx \sigma_E$ for a good fit.

Now consider χ^2 as a function of the optical parameters which are involved implicitly through σ_T . The search routine will vary these parameters automatically until a satisfactory minimum of χ^2 is obtained. The search routine will be discussed in the following section.

The elastic scattering routine (ELSCAT) will calculate the cross sections $\sigma_T(\theta_i)$. All the calculations are performed in the centre-of-mass system, in which a two-body problem can be reduced to a one-body problem.

(17)

We start from the Schroedinger equation

$$\left[-\frac{\hbar^2}{2\mu} \nabla^2 + V(r) \right] \psi(\underline{r}) = E\psi(\underline{r}). \quad (2-1)$$

The relative motion of the two particles is described completely by this equation along with the relevant boundary conditions. In the present situation the boundary conditions will be (1) that asymptotically at large distances the wave function should consist of a Coulomb-distorted plane wave and outgoing spherical waves, and (2) that the radial wave functions vanish at the origin.

Expand $\psi(\underline{r})$ in terms of the spherical harmonics

$$\psi(\underline{r}) = \sum_{\ell, m} \frac{4\pi U_{\ell}(k, r)}{kr} i^{\ell} Y_{\ell}^{m*}(\hat{k}) Y_{\ell}^m(\hat{r}), \quad (2-2)$$

where $\hbar^2 k^2 = 2\mu E$, and \hat{k} and \hat{r} are unit vectors along the directions \underline{k} and \underline{r} respectively. Substitute (2-2) into (2-1), one obtains the radial wave equations.

$$\frac{d^2 u_{\ell}}{dr^2} + \left\{ \frac{2\mu}{\hbar^2} (E - V) - \frac{\ell(\ell + 1)}{r^2} \right\} u_{\ell} = 0. \quad (2-3)$$

Rewrite this equation by introducing the dimensionless

(18)

quantities

$$\gamma = \frac{uZ_I Z_T e^2}{kh^2}, \quad \text{and } \rho = kr.$$

One has

$$\frac{d^2 u_\ell}{d\rho^2} + \left(1 - \frac{V_c(\rho)}{E} - \frac{V_n(\rho)}{E} - \frac{\ell(\ell+1)}{\rho^2} \right) u_\ell = 0. \quad (2-3)$$

The numerical integration of this equation is carried out to some distance r_{\max} where the nuclear potential is negligible. Outside of this region the interaction is the Coulomb force only. Eq.(2-3) becomes the well-known Coulomb wave equations

$$\frac{d^2 u_\ell}{d\rho^2} + \left(1 - \frac{2\gamma}{\rho} - \frac{\ell(\ell+1)}{\rho^2} \right) u_\ell = 0, \quad (2-4)$$

which are satisfied by the regular and irregular Coulomb functions $F_\ell(\gamma, \rho)$ and $G_\ell(\gamma, \rho)$. They have the following asymptotic forms at large values of ρ

$$\begin{aligned} F_\ell(\rho) &\sim \sin\left(\rho - \gamma \ln 2\rho - \frac{\ell\pi}{2} + \sigma_\ell\right) \\ G_\ell(\rho) &\sim \cos\left(\rho - \gamma \ln 2\rho - \frac{\ell\pi}{2} + \sigma_\ell\right) \end{aligned} \quad (2-5)$$

(19)

The Coulomb phase shift σ_ℓ is defined such that $F_\ell=0$ at $\rho=0$, and satisfies the recursion relation

$$\sigma_\ell = \sigma_{\ell+1} - \tan^{-1}\left(\frac{\gamma}{\ell+1}\right). \quad (2-6)$$

The combinations

$$G_\ell - iF_\ell = e^{-i(\rho - \gamma \ln 2\rho - \frac{\ell\pi}{2} + \sigma_\ell)} \quad (2-7)$$

$$G_\ell + iF_\ell = e^{i(\rho - \gamma \ln 2\rho - \frac{\ell\pi}{2} + \sigma_\ell)}$$

represent the incoming and outgoing waves respectively. The solutions of Eq.(2-4) can be written

$$u_\ell = \bar{Y}_\ell \left[(G_\ell - iF_\ell) - \eta_\ell (G_\ell + iF_\ell) \right],$$

or

$$u_\ell = Y_\ell \left[F_\ell + i\beta_\ell (G_\ell + iF_\ell) \right],$$

where

$$2\beta_\ell = 1 - \eta_\ell.$$

The scattering matrix elements β_ℓ are obtained by joining the solutions of (2-3) and (2-4). Let \bar{Y}_ℓ be the solution of Eq.(2-3), which is calculated by numerical integration of Eq.(2-3).

(20)

At matching radius r_m one has

$$F_\ell(r_m) = \gamma_\ell \left[F_\ell(r_m) + i\beta_\ell (G_\ell(r_m) + iF_\ell(r_m)) \right] \quad (2-8)$$

$$F_\ell(r_m - \delta) = \gamma_\ell \left[F_\ell(r_m - \delta) + i\beta_\ell (G_\ell(r_m - \delta) + iF_\ell(r_m - \delta)) \right],$$

where δ is a small radial increment. β_ℓ is obtained by solving the two equations. The differential cross-sections are then given by

$$\frac{d\sigma}{d\Omega} = |I(\theta)|^2,$$

where $I(\theta)$ is scattering amplitude¹¹⁾

$$I(\theta) = f_c(\theta) + \frac{i}{k} \sum_{\ell} (2\ell + 1) e^{2i\sigma_\ell} \beta_\ell P_\ell^0(\cos\theta). \quad (2-9)$$

f_c is the same as the Rutherford scattering amplitude

$$f_c(\theta) = - \frac{\gamma}{(2k) \sin^2 \frac{\theta}{2}} \exp(2i\sigma_0 - 2i\gamma \ln \sin \frac{\theta}{2}).$$

The behaviour of the Coulomb wave functions $F_\ell(\gamma, \rho)$ and $G_\ell(\gamma, \rho)$ are quite different at different regions of (γ, ρ) space, especially, when γ and ρ are small.

Different approximations should be used for different regions⁷⁾.

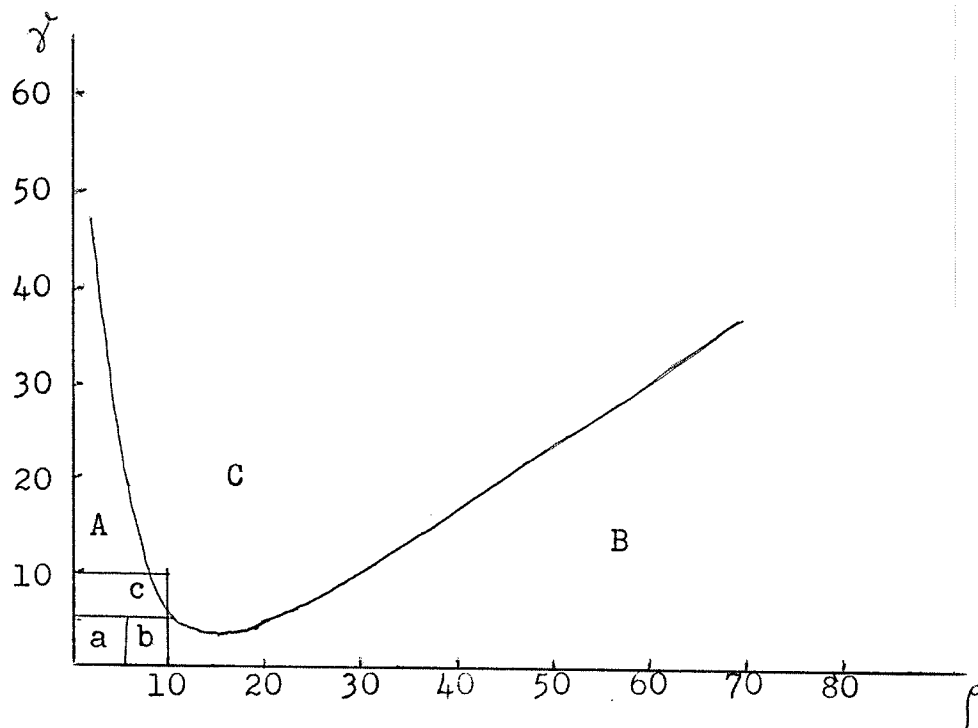


Fig. 3. Regions in which different asymptotic formulae should be used.

For the purpose of simplifying the programming and for the present problem, only method B⁷⁾ will be used. $\gamma^* = 0.63$ and $k = 2.83 \text{ fm}^{-1}$ for the $\sim 0^{16}$ scattering. In order to avoid getting into the square regions, the numerical

(22)

integration of Eq.(2-3) is carried out to a large matching radius, $r_m = 20$ fm. That corresponds to $\rho = 56.6$. This point is in the B-region in the previous diagram.

Since F_ℓ and G_ℓ are solutions of the same differential equation, they obey the same recurrence relation

$$\frac{\sqrt{\gamma^2 + (\ell+1)^2}}{\ell+1} F_{\ell+1}(\rho) + \frac{\sqrt{\gamma^2 + \ell^2}}{\ell} F_{\ell-1}(\rho) \\ = (2\ell+1) \left(\frac{\gamma}{\ell(\ell+1)} + \frac{1}{\rho} \right) F_\ell(\rho),$$

or

$$F_{\ell+1} = (B_\ell F_\ell - A_\ell F_{\ell-1}) / A_{\ell+1}, \quad (2-9)$$

where

$$A_\ell = \frac{\sqrt{\gamma^2 + \ell^2}}{\ell}, \quad \text{and} \quad B_\ell = (2\ell+1) \left[\frac{\gamma}{\ell(\ell+1)} + \frac{1}{\rho} \right].$$

F_ℓ is calculated in the downward order of ℓ by Miller's method. Since F_ℓ has the characteristic that when ℓ is larger than some value $\bar{\ell}$, the function decreases rapidly with increasing ℓ , we thus start from

$$cF_{\bar{\ell}+1} = 0.$$

(In the program this is set $cF_{\bar{\ell}+1} = 1.0 * 10^{-70}$.)

(23)

Then $cF_{\bar{\ell}} = \epsilon$. ϵ is a small number and the normalization factor c can be determined by using Eq.(2-9), it is

$$c = \frac{1}{A_{\bar{\ell}}(F_0 G_{\bar{\ell}} - F_{\bar{\ell}} G_0)} .$$

The starting value of $\bar{\ell}$ is calculated as follows:

Set $\frac{F_{\bar{\ell}}}{F_{\bar{\ell}-1}} = \frac{1}{10}$ at the first run.

The recursion formula Eq.(2-9) gives

$$\frac{F_{\bar{\ell}}}{F_{\bar{\ell}-1}} \approx \frac{A_{\bar{\ell}}}{B_{\bar{\ell}}} \approx \frac{\gamma^2 + \bar{\ell}^2}{2\bar{\ell}^2(\frac{\gamma}{\rho} + \frac{1}{\rho})} = \frac{1}{10} .$$

Solving for $\bar{\ell}$, one obtains

$$\bar{\ell} = \sqrt{\frac{\rho}{2}} \left\{ 25 - \frac{2\gamma}{\rho} + 10 \sqrt{\left(\frac{\gamma}{\rho} - \frac{1}{2}\right)^2 + 6} \right\}^{\frac{1}{2}} .$$

To check on the error, $\bar{\ell}$ is then replaced by $\ell' = \bar{\ell} + 10$, and repeat the calculation. If the difference between the ratios $F_{\ell'}/F_0$ is less than 0.01%, then the last $cF_{\ell'}$ value

(24)

will be used in the following calculations. Otherwise the program will repeat the previous procedure again and increases $\bar{\ell}$ by 10 each time until a satisfactory value of ℓ is obtained.

The irregular Coulomb wave function G_ℓ is calculated by recursion upward in ℓ and inward in r . The values of G_0 and G_1 are obtained asymptotically at large ρ^7 .

Define

$$D_n = \frac{(2n+1)\gamma}{2(n+1)\rho}, \quad E_n^\ell = \frac{\ell(\ell+1) - n(n+1) + \gamma^2}{2(n+1)\rho}.$$

They satisfy the relations

$$s_{n+1} = D_n s_n - E_n^\ell t_n \tag{2-10}$$

$$t_{n+1} = D_n t_n + E_n^\ell s_n,$$

with the initial conditions $s_0 = 1$ and $t_0 = 0$.

Put

$$s = \sum s_n, \quad t = \sum t_n.$$

(25)

The summations of these divergent series are cut off after a suitable number of terms ($n=15$). The asymptotic formulae of Coulomb wave functions are

$$F_l = t \cos \theta_l + s \sin \theta_l \quad (2-11)$$

$$G_l = s \cos \theta_l - t \sin \theta_l ,$$

where $\theta_l = \rho - \gamma \ln 2\rho - \frac{l\pi}{2} + \sigma_l$.

To check the dependability of the calculation, set $V_n=0$, the radial wave functions are then the linear combinations of the Coulomb functions.

Eq.(2-3) is integrated numerically by employing the quadratic interpolation and the Schroedinger equation

$$\begin{aligned} & \left[\mathcal{F}_l(r+\delta) - 2\mathcal{F}_l(r) + \mathcal{F}_l(r-\delta) \right] / \delta^2 \\ & \simeq \left[\mathcal{F}_l''(r+\delta) + 10\mathcal{F}_l''(r) + \mathcal{F}_l''(r-\delta) \right] / 12 \end{aligned} \quad (2-12)$$

Put $Q_l(r) = 1 + \frac{\delta^2}{12} \left[k^2 - \frac{2\mu V(r)}{\hbar^2} - \frac{l(l+1)}{r^2} \right]$, (2-13)

where $V(r) = V_c + V_n$. Combine Eq.(2-3), (2-12), and (2-13),

(26)

one obtains the recursion formula

$$F_\ell(r+\delta) = \left[(12 - 10Q_\ell(r))F_\ell(r) - Q_\ell(r-\delta)F_\ell(r-\delta) \right] / Q_\ell(r+\delta). \quad (2-14)$$

The normalization factor Y_ℓ of F_ℓ is not important, because the first equation of Eq. (2-8) is divided by the second one and Y_ℓ is cancelled out. The recurrence in Y_ℓ is started from the following values:

$$F_\ell(-\delta) = 0, \quad Q_\ell(-\delta) = 0, \quad F_\ell(0) = \delta^{(\ell+1)}(1+i),$$

$$Q_\ell(0) = 0.$$

These are to satisfy the second boundary condition of Eq. (2-1).

2-2 AUTOMATIC SEARCH ROUTINE

(A) Normal Equation Method

The search routine is designed to find the optical parameters which correspond to good fit to the experimental angular distributions. This is to minimize the quantity χ^2 . In order to standardize this quantity, we then divide χ^2 by N , the total number of experimental points.

$$\chi^2 = \frac{1}{N} \sum_i \left(\frac{\sigma_T(\theta_i) - \sigma_E(\theta_i)}{\delta\sigma_E(\theta_i)} \right)^2. \quad (2-15)$$

Put $\chi^2 = f(x_1, x_2, \dots)$, where x_i 's represent the optical parameters to be determined. Assume f has a minimum at

$$x_i(M) = x_i(0) + \Delta x_i, \quad (i=1, 2, \dots)$$

where M indicates the minimum, and 0 , the starting point in the parameter space. The sufficient conditions for a minimum are

$$\left(\frac{\partial f}{\partial x_i} \right)_M = 0 \quad (2-16)$$

From Eq.(2-16) a set of linear equations of x_i can be deduced by assuming that the starting point 0 is sufficiently near the minimum M .

(28)

$$\begin{aligned}
\left(\frac{\partial f}{\partial x_j}\right)_M &= \left(\frac{\partial f}{\partial x_j}\right)_{x_j(0)+x_j} = 2 \sum \left(\frac{\sigma_T - \sigma_E}{(\delta\sigma_E)^2}\right)_M \left(\frac{\partial\sigma_T}{\partial x_j}\right)_M \\
&= 2 \sum \left\{ \left[(\sigma_T - \sigma_E)_0 + \left(\sum_k \left(\frac{\partial\sigma_T}{\partial x_k}\right)_0 \Delta x_k \right) \right. \right. \\
&\quad \left. \left. + (\text{2nd order terms of } \Delta x) \right] \cdot \left(\frac{\partial\sigma_T}{\partial x_j}\right)_M \cdot \left(\frac{1}{\delta\sigma_E}\right)^2 \right\} = 0, \\
&\qquad\qquad\qquad (j=1,2,\dots) \qquad (2-17)
\end{aligned}$$

Neglecting the second-order terms, Eq.(2-17) can be rewritten as

$$\begin{aligned}
\sum_{i=1}^N \frac{1}{(\delta\sigma_E)^2} \left[\sum_k \left(\frac{\partial\sigma_T}{\partial x_k}\right)_0 \Delta x_k + (\sigma_T - \sigma_E) \right] \left(\frac{\partial\sigma_T}{\partial x_j}\right)_M = 0, \\
(j=1,2,\dots). \qquad (2-18)
\end{aligned}$$

Eq.(2-18) provides a set of simultaneous equations which can be solved for Δx . The derivatives are obtained numerically by the approximations

$$\frac{\partial\sigma_T}{\partial x_j} = \frac{\sigma_T(x_j + \delta x_j) - \sigma_T(x_j)}{\delta x_j} \qquad (2-19)$$

All $\left(\frac{\partial\sigma_T}{\partial x_j}\right)_M$ are replaced by $\left(\frac{\partial\sigma_T}{\partial x_j}\right)_0$, because 0 is assumed to be at the neighborhood of M. The rest of the problem is

to solve the simultaneous equations (2-18). This can be done by using IBM library subroutine.

It is apparent that the normal equation method is valid only when the starting point 0 is reasonably near the minimum. Otherwise the search becomes unstable. This is illustrated in Fig. 3. The initial values of the parameters are $r=r'=1.20$ fm, $a=a'=0.30$ fm, $U=150.0$ Mev, $W_v=16.0$ Mev, and $W_s=0.0$ Mev. The search jumped to the negative parameter space from the second to eleventh cycles.

To test the dependability of this program a different automatic search program illustrated in the next section was used to do the search starting from the same values of parameters. The differences between the optimum values of the optical parameters were within 2%.

	$r=r'$ fm	$a=a'$ fm	U(Mev)	W_v (Mev)	$\frac{d\sigma}{d\Omega}$ at $32.38 \frac{6}{51}$
Normal Equation Method	1.327	0.56	251.16	88.46	32.19
Pehl-Wilkins Method	1.308	0.57	251.24	88.31	32.02
Starting Values	1.316	0.54	250.93	90.00	

(30)

Fig. 3

Unstable Three Parameter Search.

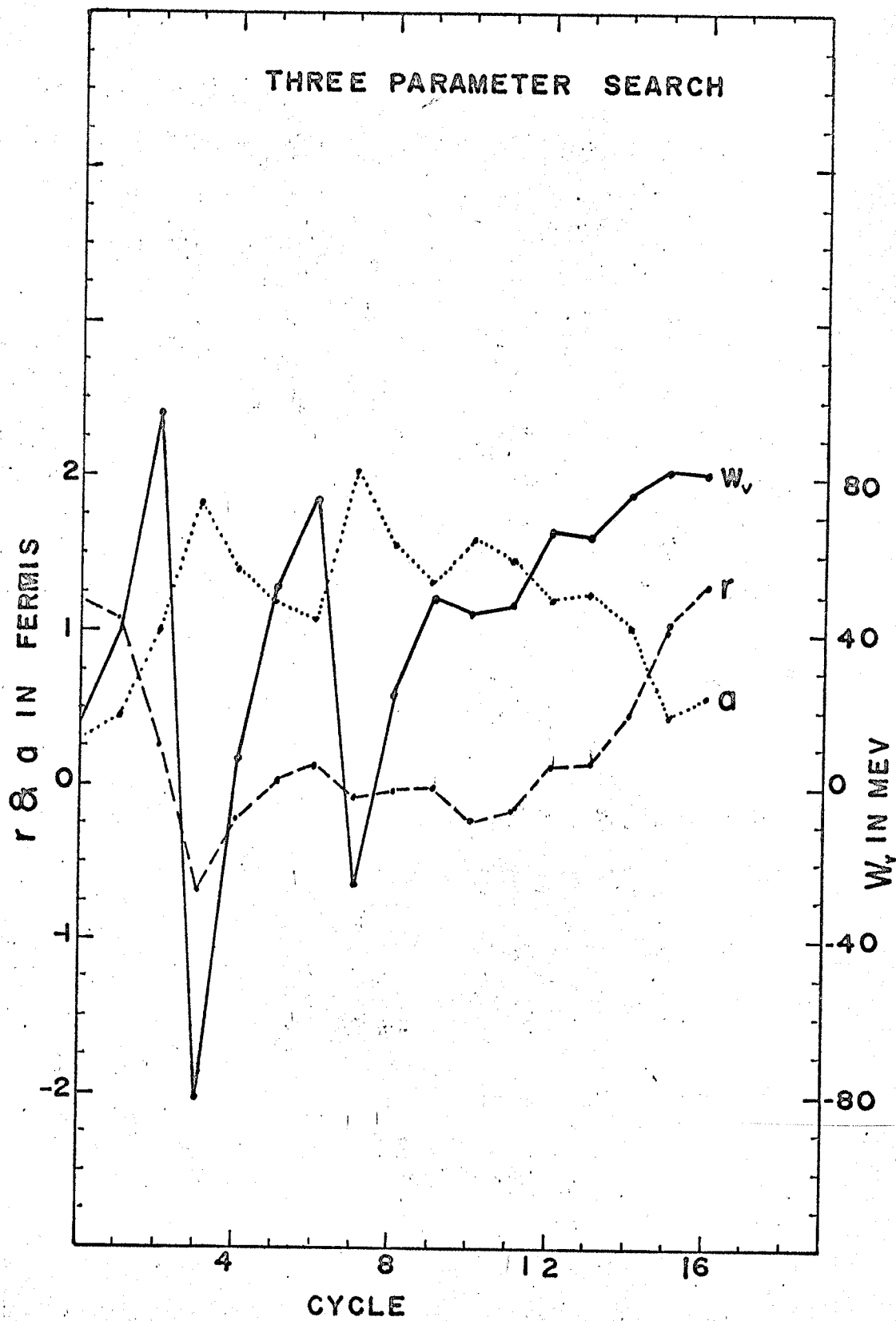


Fig. 3

(B) Pehl and Wilkins Method

It is difficult in computer programming to find a proper increment Δx for evaluation of the derivatives of a particular function f ,

$$\frac{\partial f}{\partial x} \approx \frac{f(x+\Delta x) - f(x)}{\Delta x} .$$

If Δx is too small, the calculated $\frac{\partial f}{\partial x}$ will not be correct due to the errors generated by the computer itself, and it might cause computer overflow. Pehl and Wilkins tried to free from these troubles by using the following procedure:

Define

$$G_i = \frac{f(x_i + \Delta x_i) - f(x_i)}{f(x_i)} \equiv \frac{\Delta f(x_i)}{f(x_i)} .$$

The direction toward the minimum is determined by the sign of

$$- \frac{1}{f} \frac{\Delta f(x_i)}{\Delta x_i} , \quad (f > 0) .$$

The length of a step for the variable x_i is

$$\sqrt{\frac{\frac{1}{f} \frac{\partial f}{\partial x_i}}{\sum_i \frac{1}{f} \frac{\partial f}{\partial x_i}}} * \Delta x_i * 0.01 = \sqrt{\frac{\frac{\partial f}{\partial x_i}}{\sum_i \frac{\partial f}{\partial x_i}}} * 0.01 \Delta x_i .$$

In our modification of the program, since convergence was

very slow, suitable increments were estimated at the start. If during five iterations the sign of $\frac{1}{f} \frac{\partial f}{\partial x}$ remains the same the increment is doubled. Conversely, once the derivative changes its sign, the increment is reduced by half so that the search will converge right at the bottom of the valley. The computer stops searching for the optimum value of x_i when

$$\frac{\Delta x_i}{x_i} \leq 0.01 .$$

The search is considered complete when all the parameters satisfied this requirement. The standard may be changed to meet the demand of a particular problem.

This automatic search routine does not involve the assumption that the starting point should be near the minimum. It will converge to the nearest minimum if the calculation is started with markedly different values of optical parameters. This is very helpful for the systematic analysis of parameter ambiguities. One of the convergence searches is shown in Fig. 4.

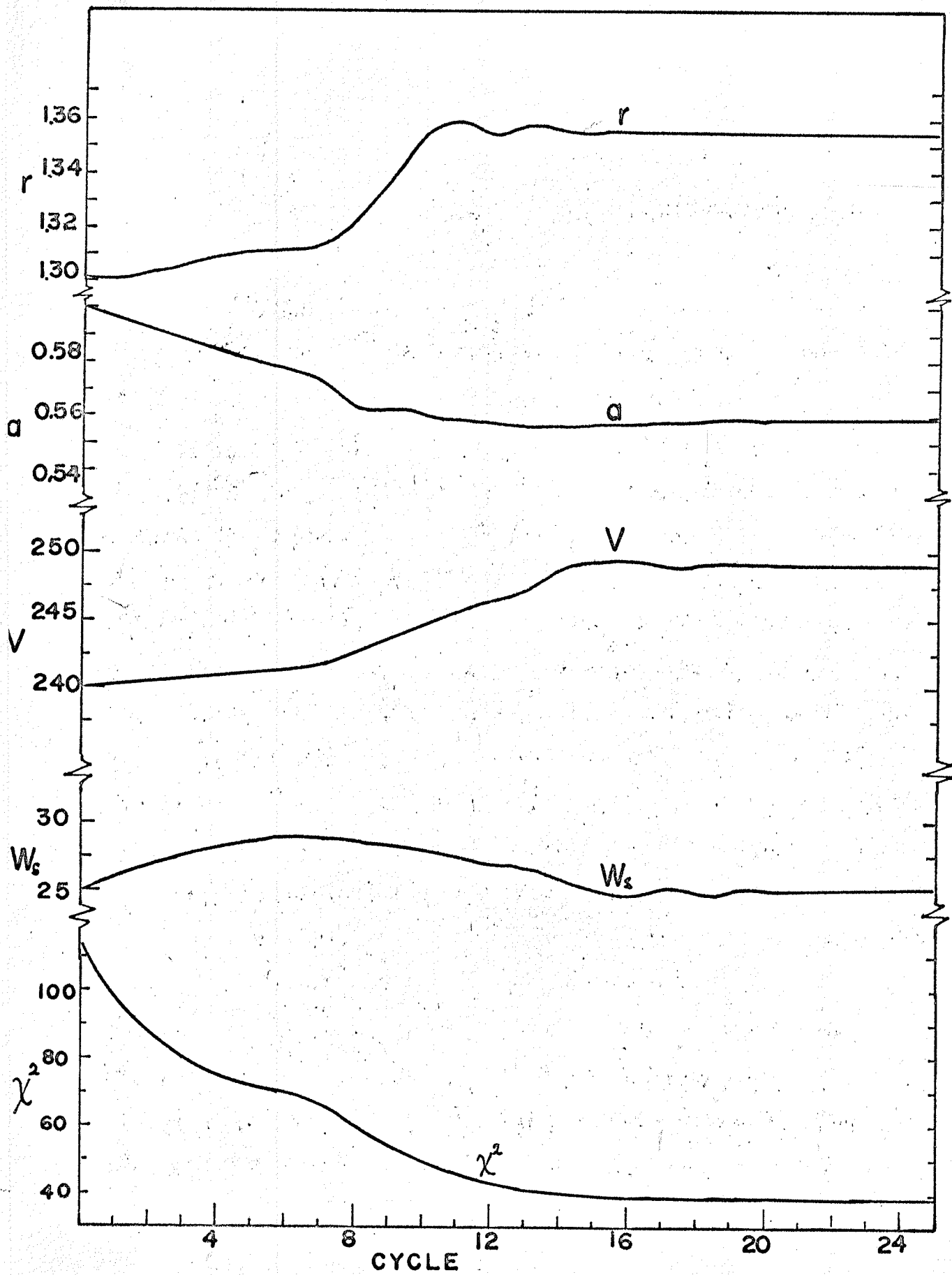


Fig. 4

CHAPTER III

OPTICAL MODEL POTENTIALS AND PARAMETER AMBIGUITY

3-1 $\propto 10^{-16}$ Optical Model Potentials

The experimental differential cross-sections have been fitted using surface absorption term for the imaginary part of the potential. The program was normally run for around 30 cycles to satisfy the conditions for convergence. This depends on the separations between the starting values and the optimum values of the optical parameters. The Coulomb radius parameter r_c was fixed at 1.4 fm. The sensitiveness of the calculated differential cross-sections to the variation of r_c will be discussed later. Primary searches were started from various points in the parameter space to obtain the whole set of minima of χ^2 corresponding to good fit. In order to get the approximate separation between the successive minima, the starting values were as follows:

the real depth $V=60$ to 300 MeV with 10 MeV spacing,
and the geometrical parameters are

$$r_0 = r'_0 = 1.2 \text{ fm}, a = a' = 0.6 \text{ fm}, W_s = 20 \text{ MeV}.$$

The parameters representing all the converged searches are listed in Table 2. There are gaps between $V=249$ MeV and 198 MeV, and $V=136$ and 75 MeV. The searches were very unstable

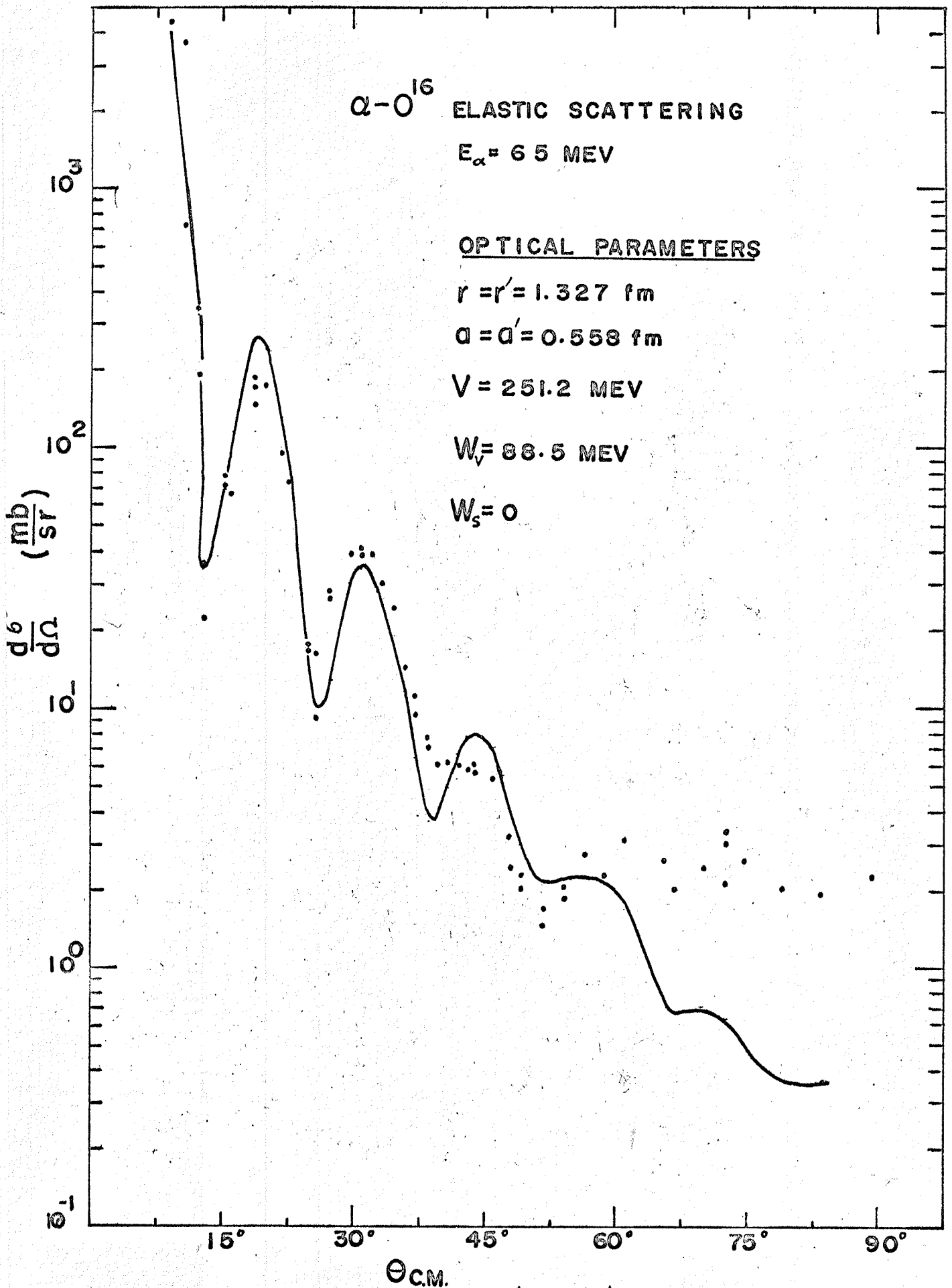
	V (Mev)	$r_0=r'_0$ (fm)	$a=a'$ (fm)	W_s (Mev)	2	Vr_0^2	
1	305.2	1.177	0.625	29.4	34	423	} I
2	288.0	1.209	0.618	27.1	27	422	
3	275.2	1.258	0.598	26.2	30	435	
4	256.9	1.320	0.572	25.8	35	447	
5	249.1	1.355	0.559	25.0	39	457	
	(gap)	-	-	-	-	-	
6	198.3	1.244	0.645	22.4	30	307	} II
7	172.6	1.385	0.586	20.3	42	331	
8	135.8	1.251	0.705	18.2	47	212	III
	(gap)	-	-	-	-	-	
9	75.0	1.420	0.668	16.9	88	151	IV

Table 2. $\propto -0^{16}$ Optical Potentials.

(36)

Fig. 5

Optical Model Fit Using Volume Absorption.
 $W_v = 88.5$ Mev.



(Fig. 5)

(37)

Fig. 6

Optical Model Fit Using Surface Absorption

$$r = r' = 1.177 \text{ fm}$$

$$a = a' = 0.625 \text{ fm}$$

$$V = 305.2 \text{ Mev}$$

$$W_s = 29.4 \text{ Mev}$$

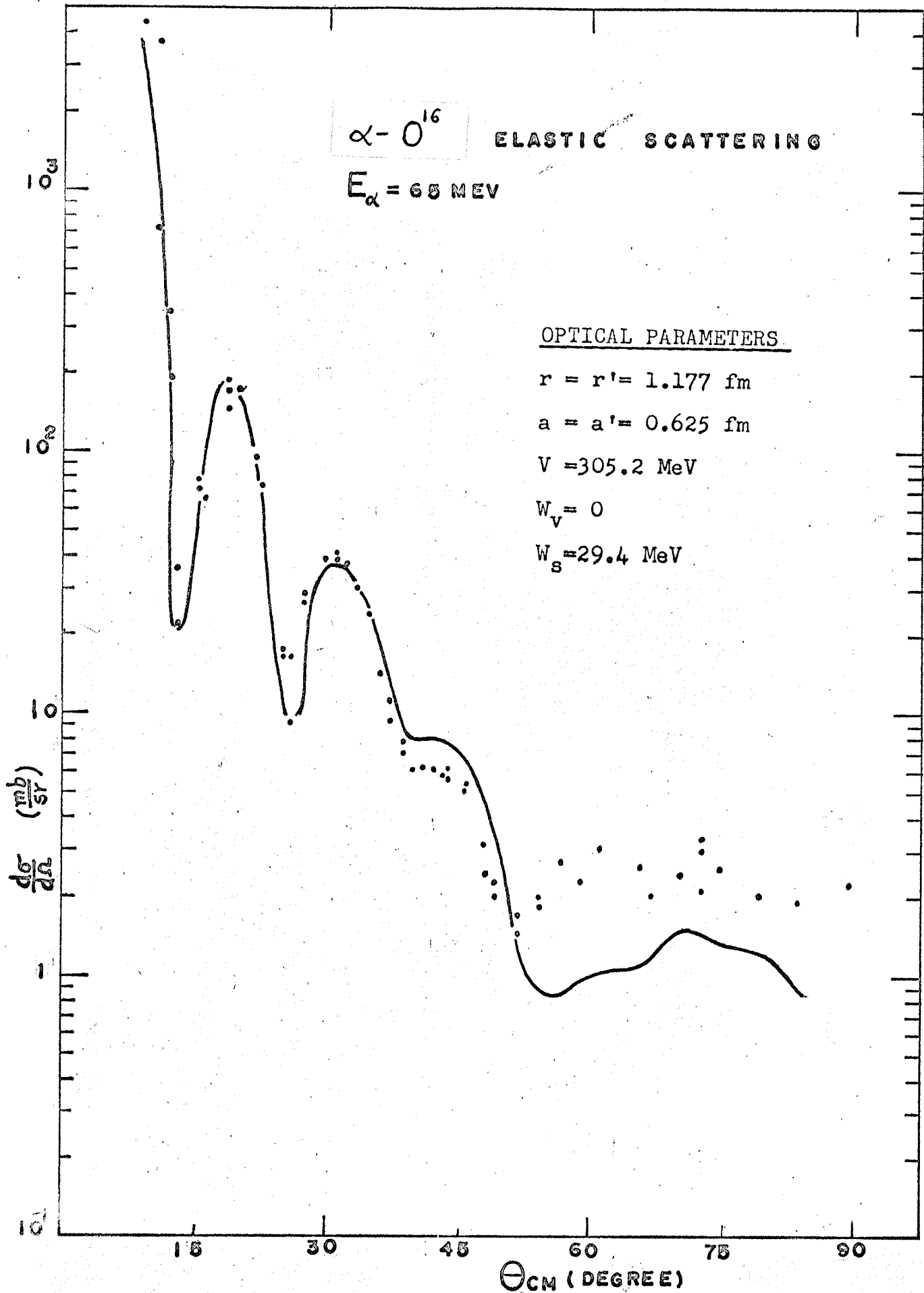
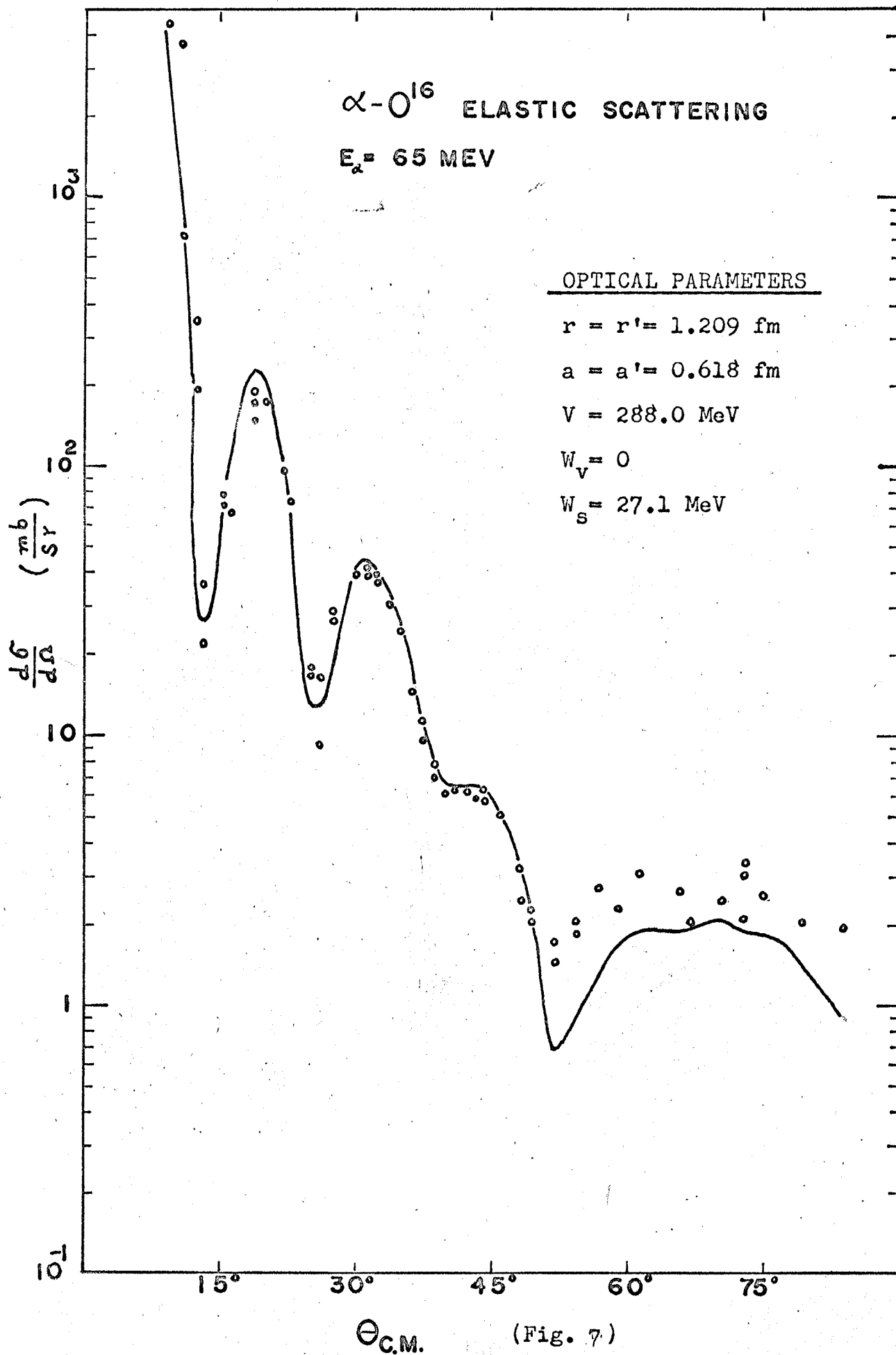


Fig. 7

Optical Model Fit, $V=288.0$ Mev, $W_s=27.1$ Mev. It gives excellent fit to the experimental point at angles around 45° .

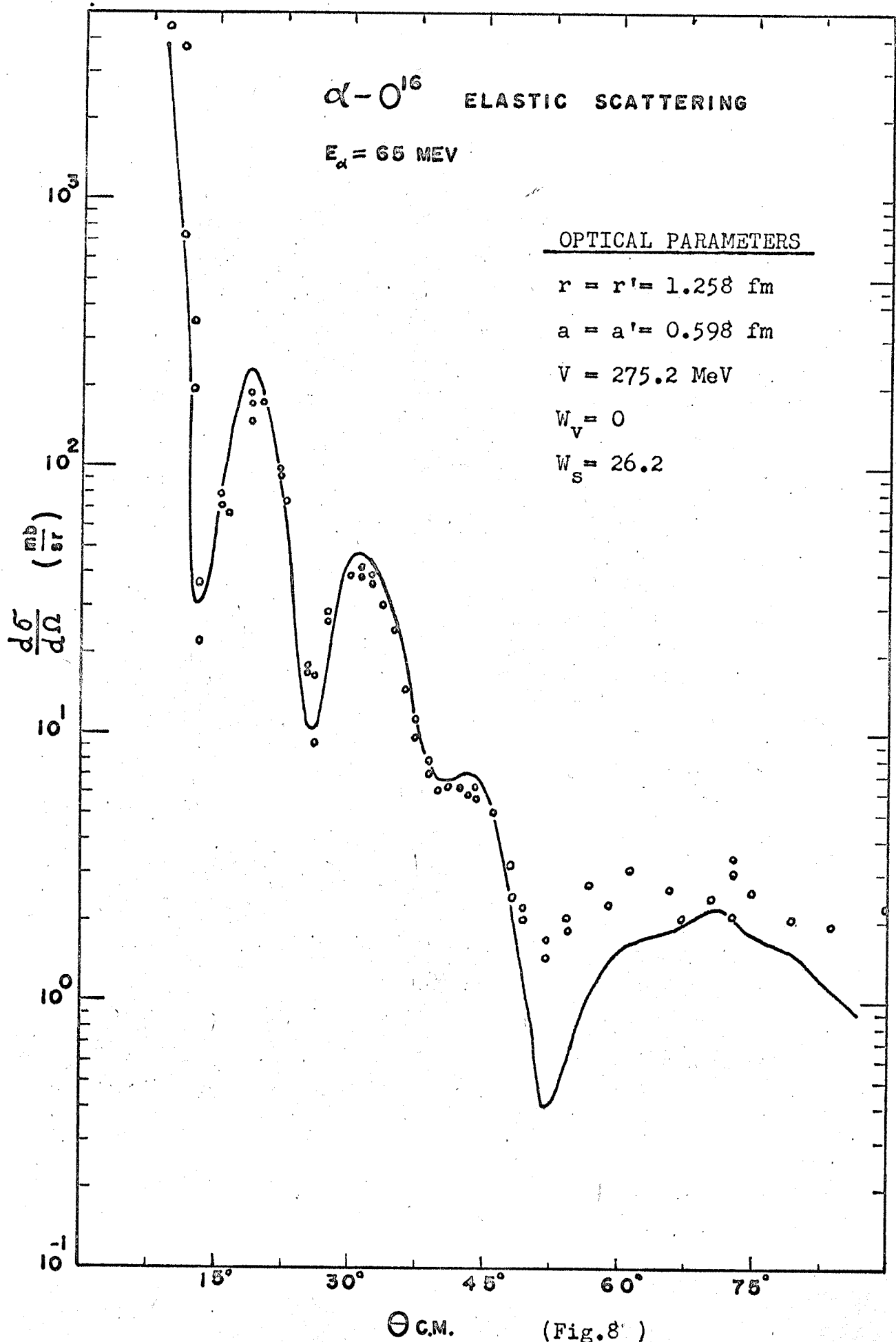


(Fig. 7)

(39)

Fig. 8

Optical Model Fit, $V = 275.2$ Mev, $W_s = 26.2$ Mev.



(40)

Fig. 9

Optical Model Fit, $V = 256.9$ Mev, $W_s = 25.8$ Mev.

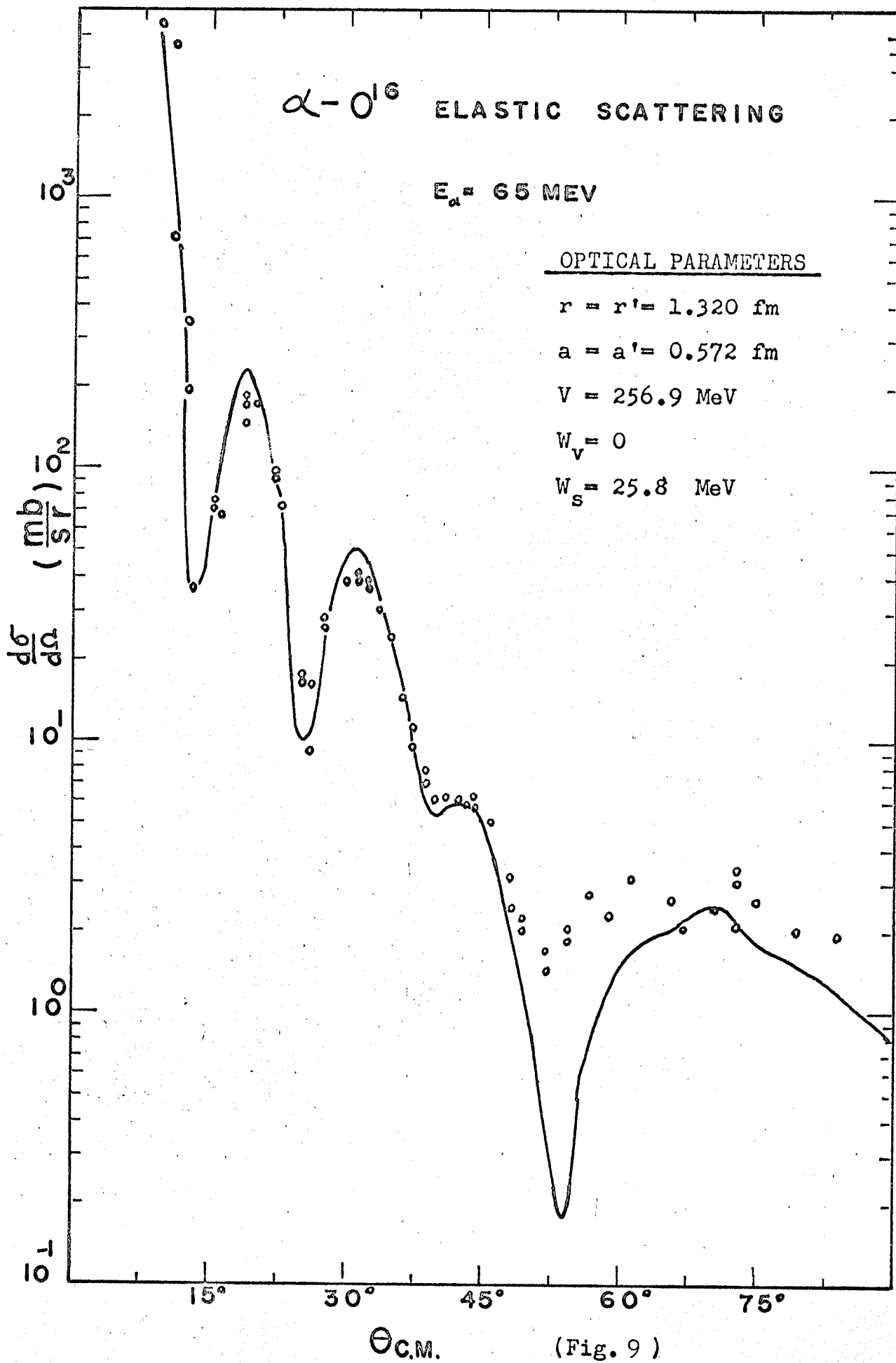


(Fig. 9)

(41)

Fig. 10

Optical Model Fit, $V = 249.1$ Mev, $W_s = 25.0$ Mev.

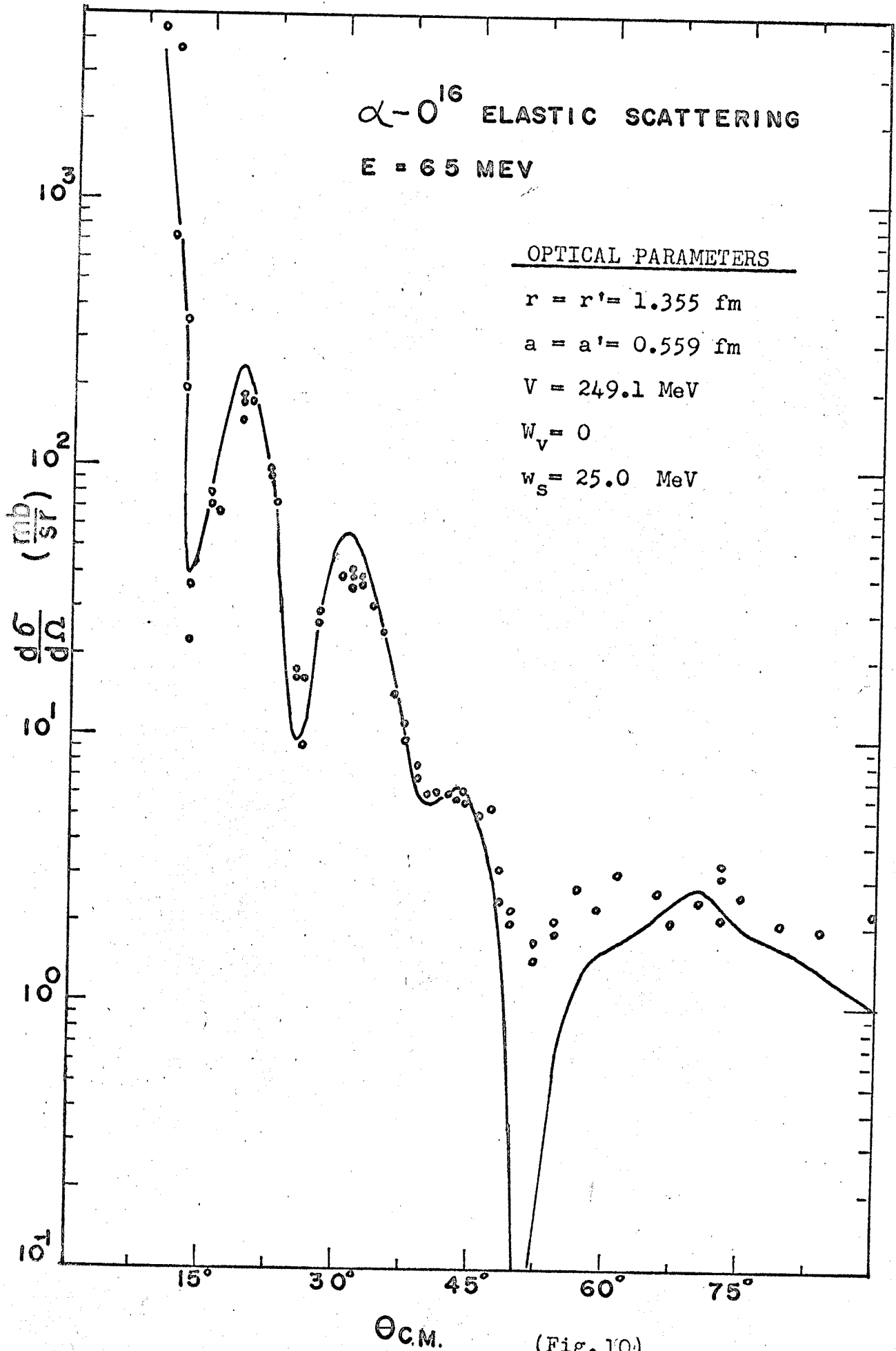


(Fig. 10)

(42)

Fig. 11

Optical Model Fit, $V = 198.3$ Mev, $W_s = 22.36$ mev.

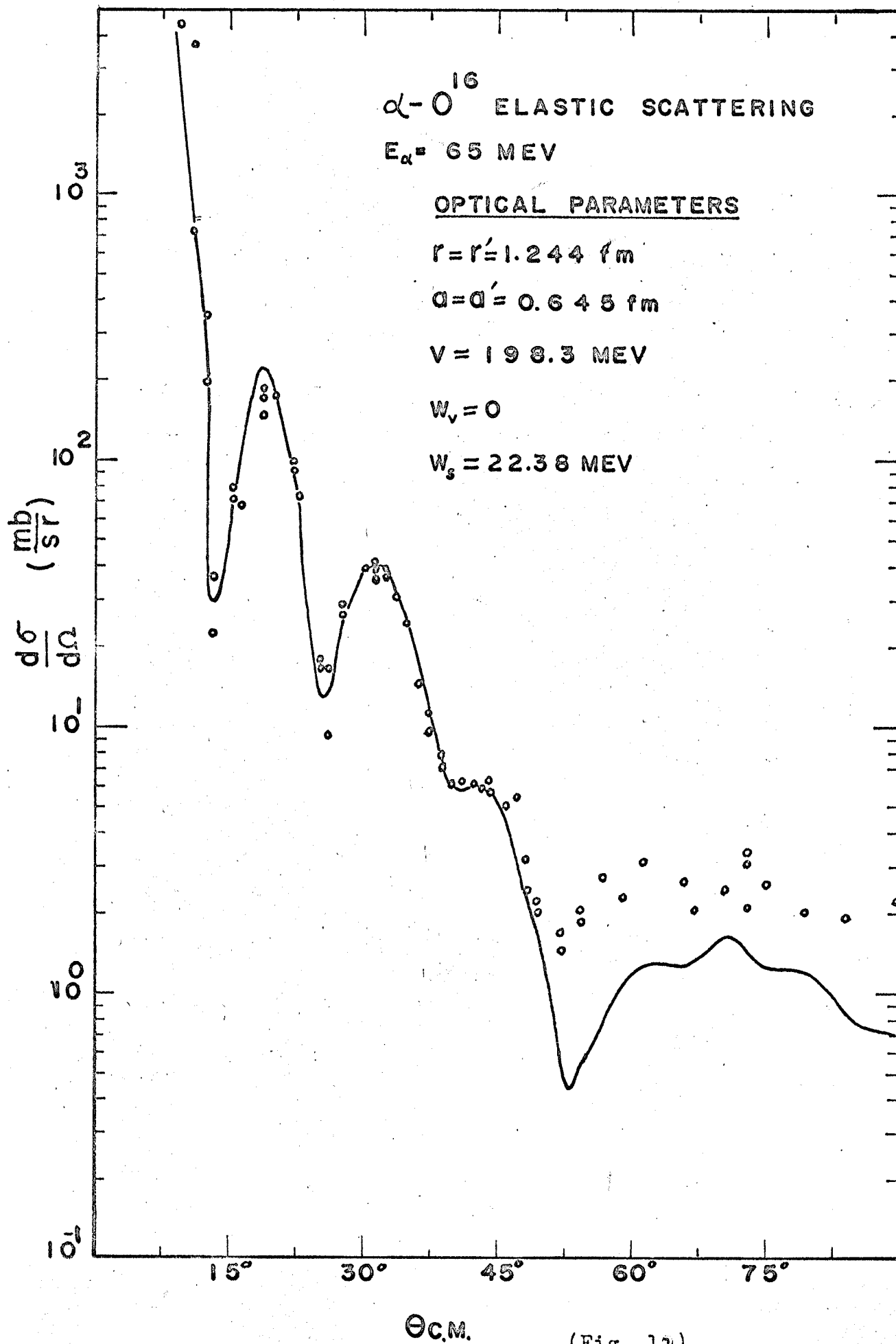


(Fig. 11)

(43)

Fig. 12

Optical Model Fit, $V = 172.6$ Mev, $W_S = 20.26$ Mev.

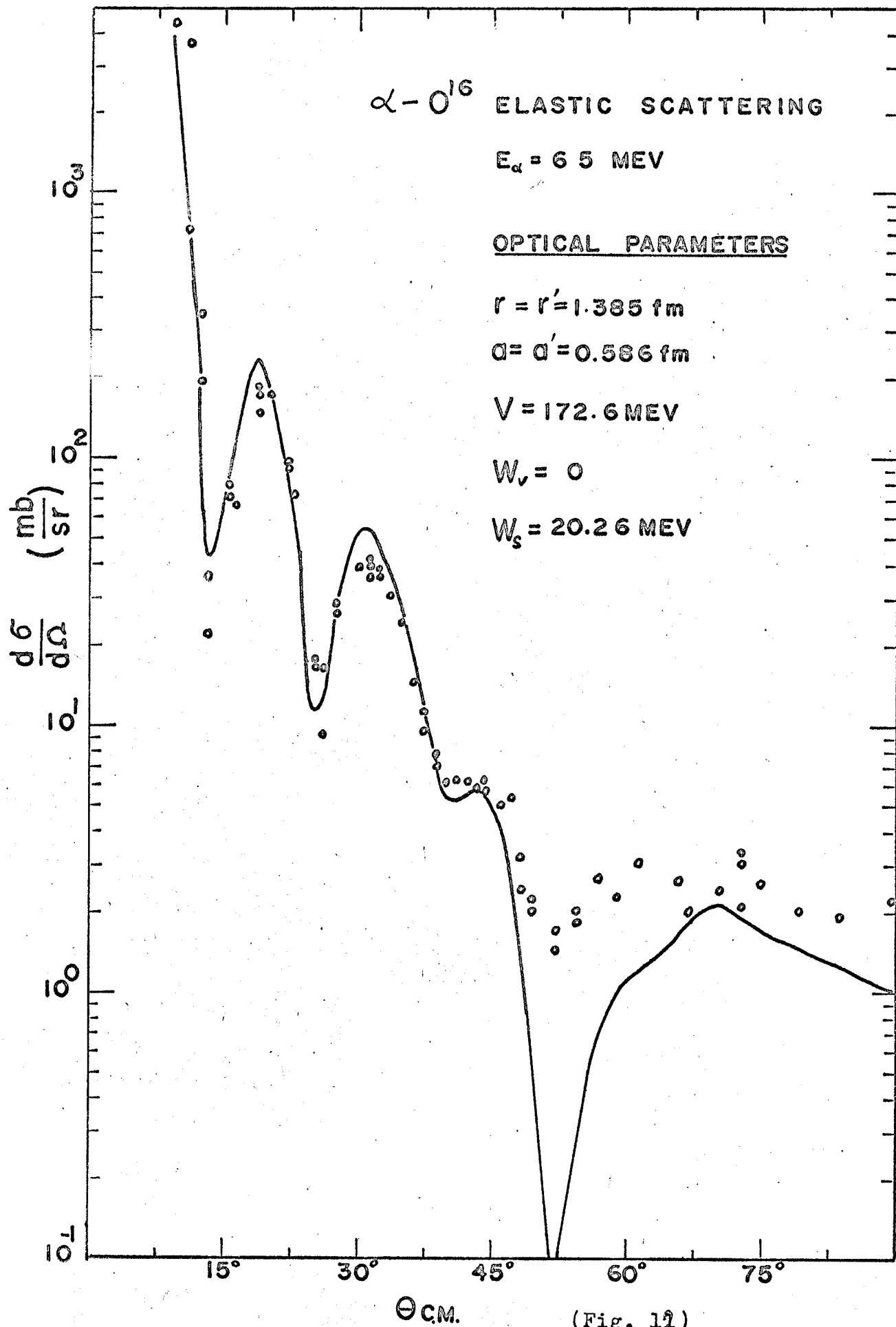


(Fig. 11)

(44)

Fig. 13

Optical Model Fit, $V = 135.8$ Mev, $W_s = 18.2$ Mev.
The fitting is relatively poor at large angles
using a shallow potential.

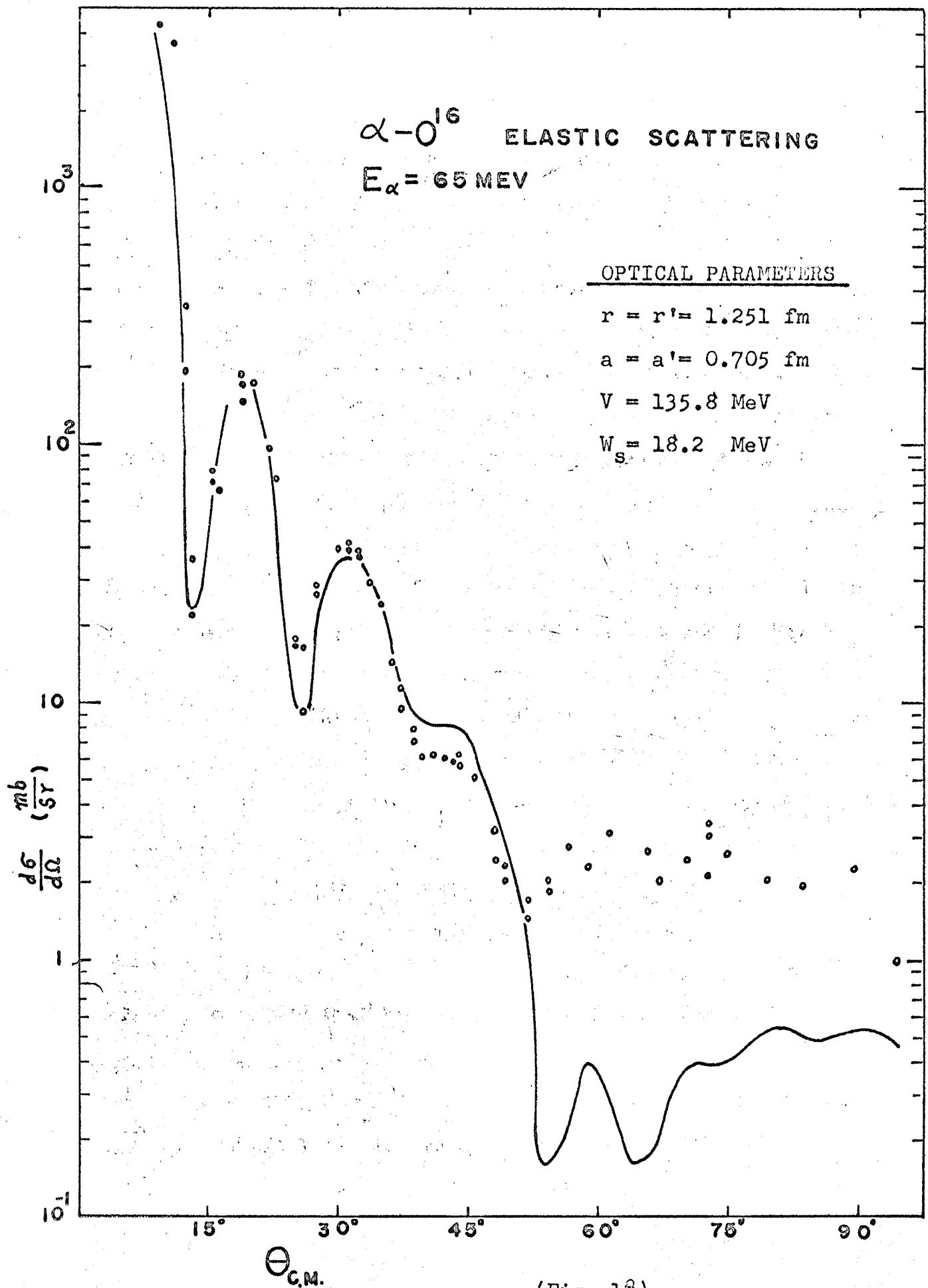


(Fig. 13)

and no minima had been found within these gaps. The fittings are shown in Fig. 5-12.

The arguments and moduli of η_ℓ corresponding to the convergent searches are shown in Fig. 13 and 14. All the magnitudes of η_ℓ converge to unity around $\ell=20$. This indicates that the partial waves with $\ell > 20$ are not important. The number of partial waves taking into consideration was set equal to 25 throughout the analyses.

The radial wavefunctions for $\ell=0, 1, \text{ and } 2$ corresponding to the potentials (1) and (2) in Table 2 are plotted in Fig. 15 and Fig. 16. It can be expected that the amplitudes of the wavefunctions inside the nucleus should be larger for smaller absorptions, i.e., for smaller value of W . According to the model, a nucleus acts partly as a particle-sink, the probability density of the incident particle inside the nucleus is thus larger for smaller absorptions.

The fittings are good to about $\theta_{\text{cm}} = 50^\circ$. The deviations between the theory and the experiment increase after $\theta_{\text{cm}} = 50^\circ$ partly due to increasing statistical errors at large angles. The scattering seems to be in favor of the potential with deeper wells. The potentials (2) to (5) in

Table 2 give better overall fits, while the deepest and shallowest give poorer fits. We thus expect that there will be no optimum point in the parameter space outside of this region.

Fig. 5 shows one of the fittings using volume absorption term for the imaginary part of the potential. The feature of fitting illustrates that the optical model potentials with volume absorption are not able to reproduce the damped oscillation of the angular distributions around $\theta_{cm} = 44^\circ$, and give relatively poor fit at large angles. Only the surface absorption gives good account for these regions. This indicates that the interactions near the nuclear surface are more important for the α -particle elastic scattering.

The Coulomb radius parameter r_c is varied from 0.1 to 2.0 fm. There is no practical change in the differential cross-sections. This is shown in Fig. 20. r_c is thus fixed at 1.4 fm in the actual calculation.

(47)

Fig. 14-A

Scattering Coefficients

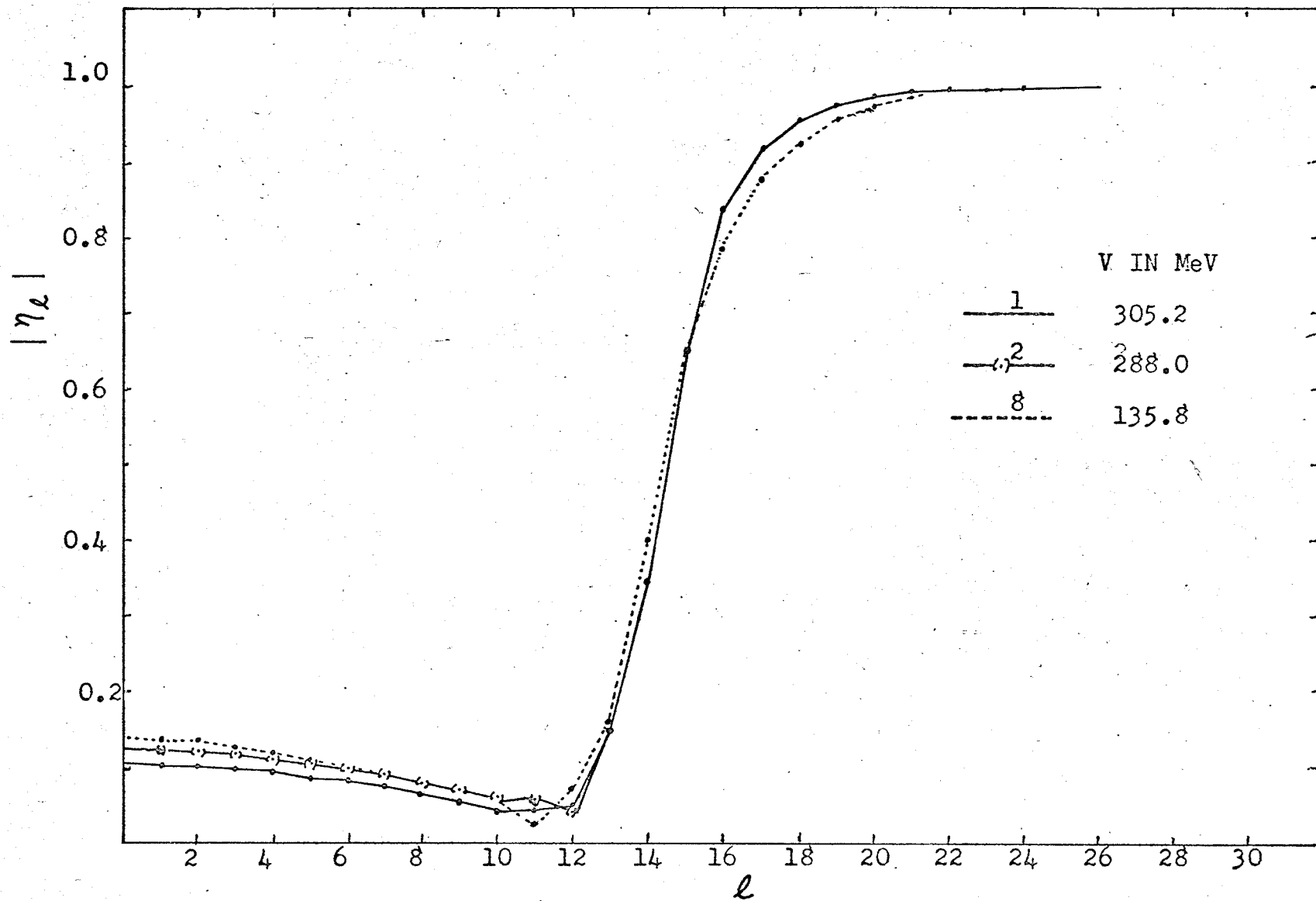


Fig. 14-A

(48)

Fig. 14 - β

The Phase of η_l

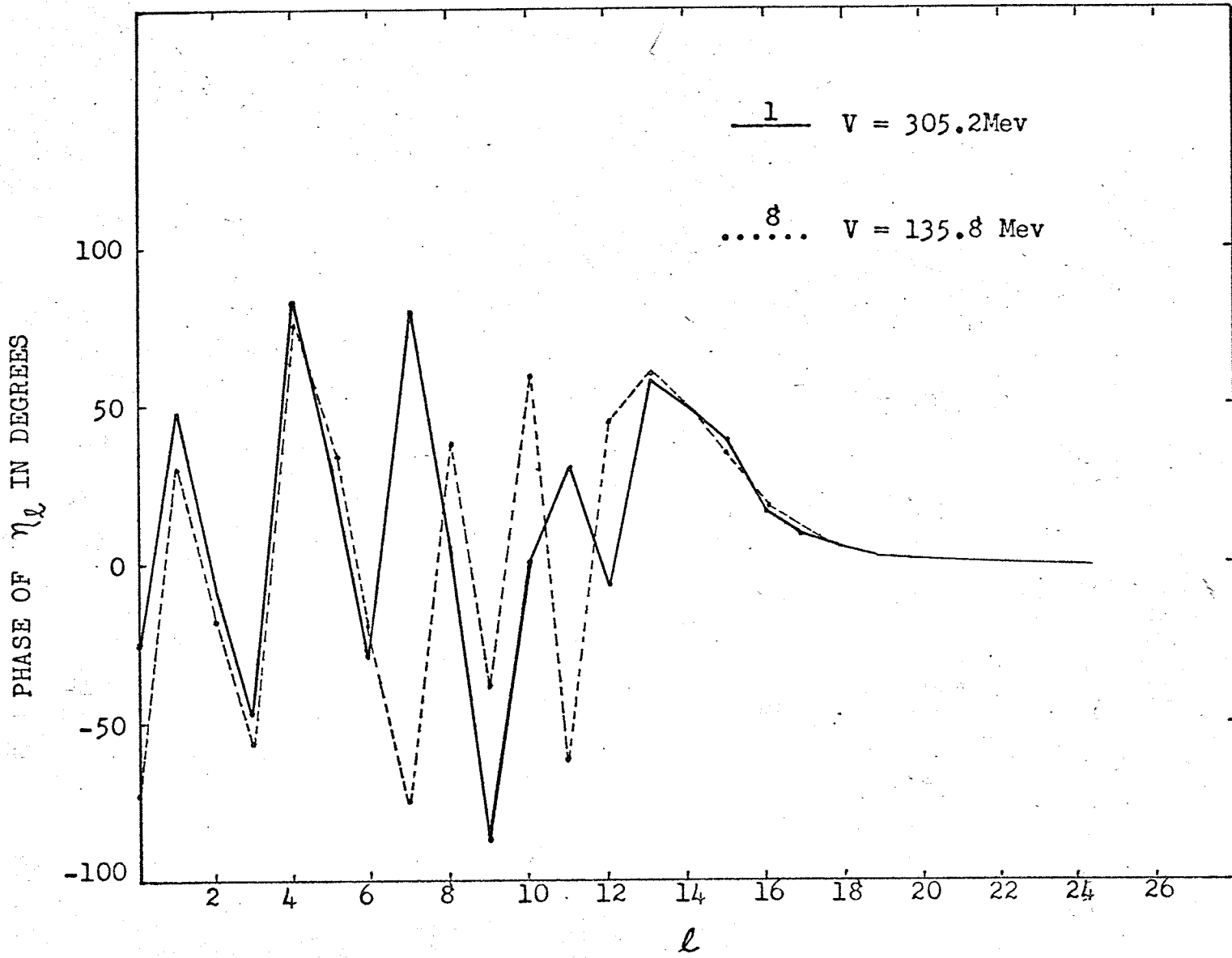
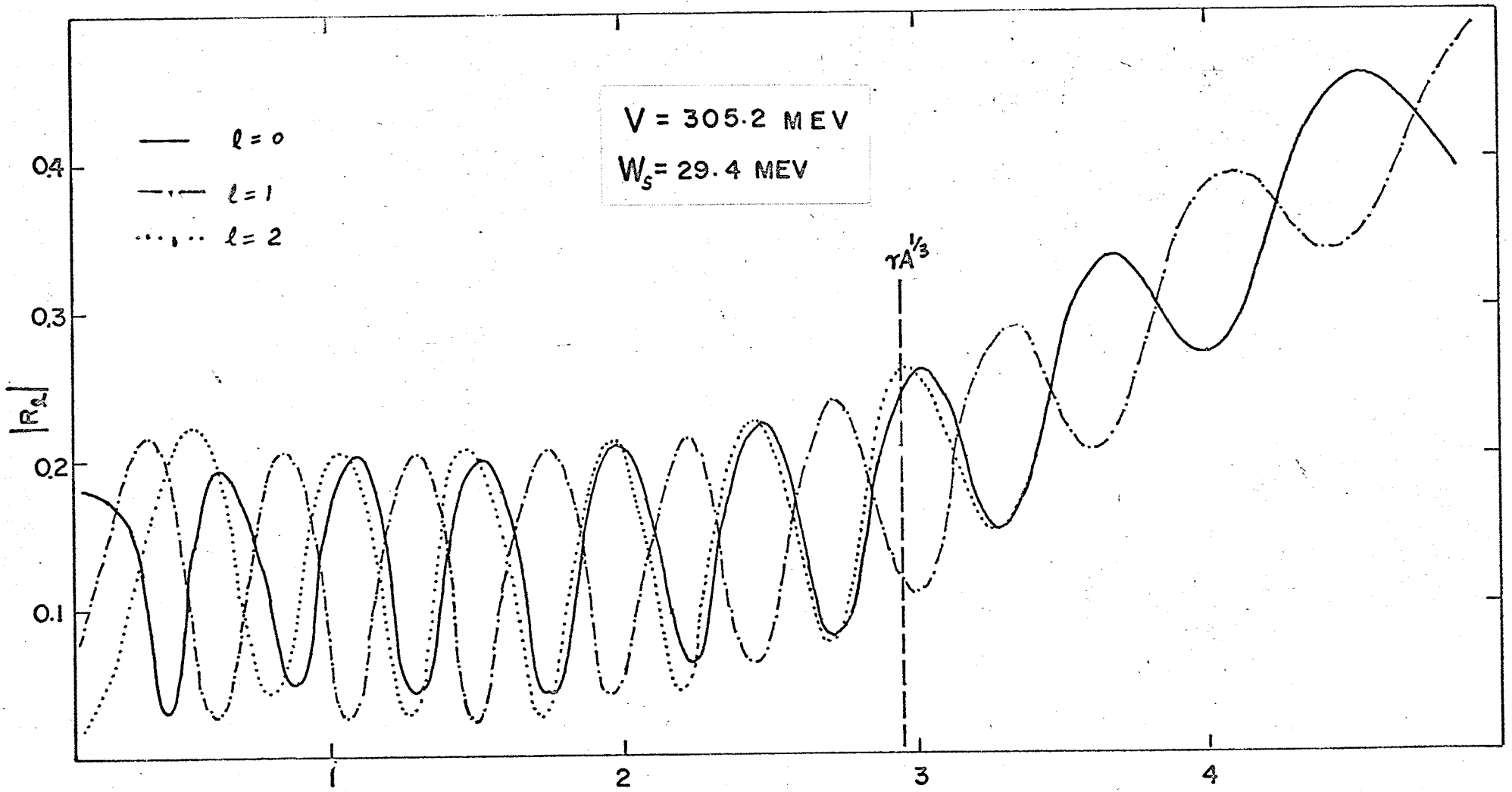


Fig. 14-B

(49)

Fig. 15

The Amplitudes of the Radial Wavefunctions for $l=0, 1, \text{ and } 2.$



(Fig.15)

(50)

Fig. 16

The Amplitudes of the Radial Wavefunctions. $V = 198.3$ Mev,

$W_s = 22.4$ Mev.

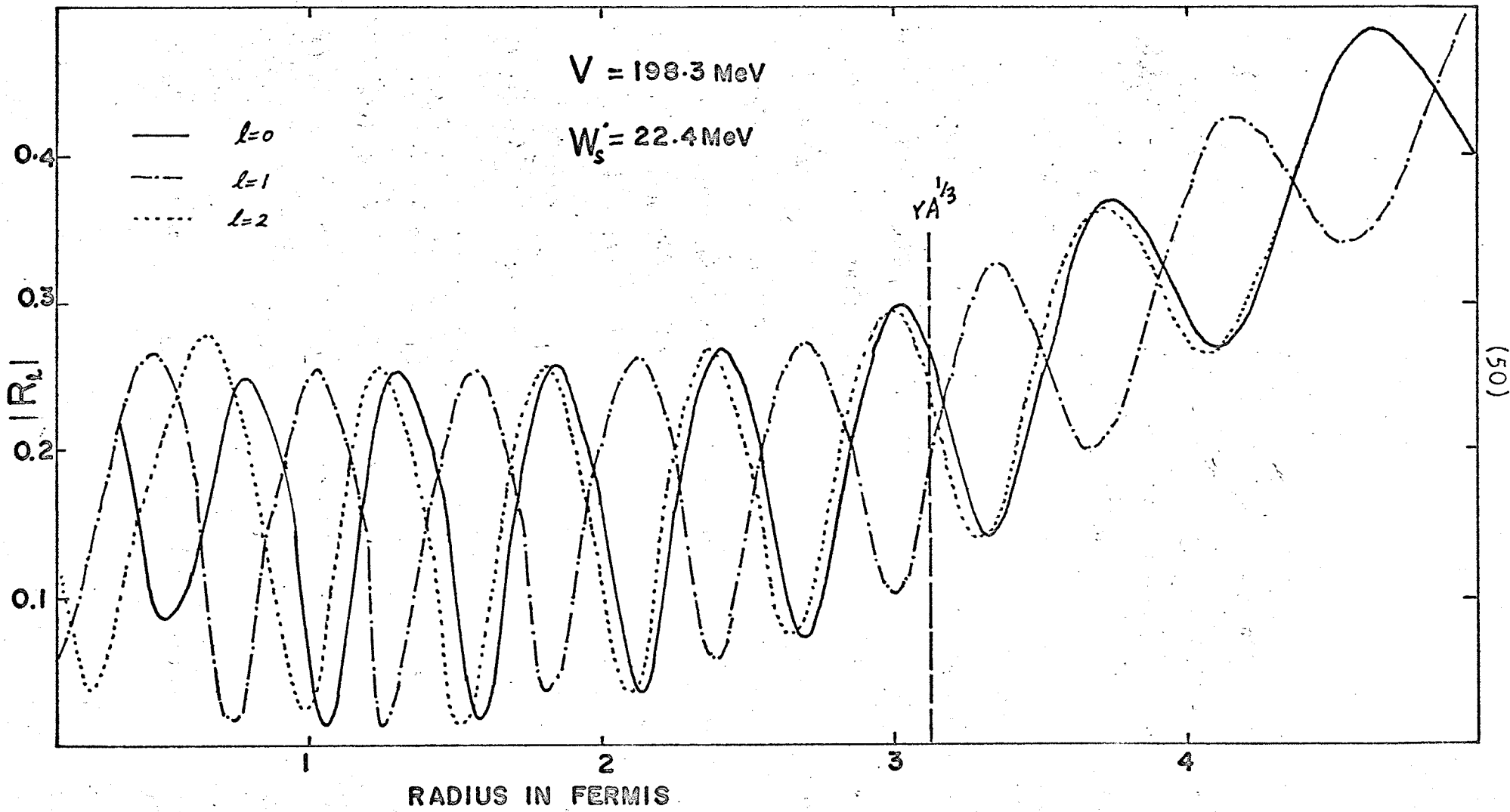


(Fig. 16)

3-2 Optical-Parameter Ambiguities

The potential obtained by the optical model analysis is not unique. All the potentials listed in Table 2 reproduce the experimental differential cross-sections reasonably well. The systematic behaviour of the parameters will be discussed in the following.

The radial wavefunctions for the s-wave corresponding the optimum potentials are shown in Fig. (17), (18), and (19). All of them have similar amplitudes and phases outside of the nuclear field. In fact, from Section (2-1), the scattering matrix elements β_l corresponding to different potentials will be the same so long as they reproduce the same asymptotic wavefunctions, regardless of the details of the wavefunctions inside the nuclear field. Thus, which potential represents the actual interaction is not resolvable solely by means of the elastic scattering experiment.

The systematics of the variation of the parameters can be divided into two categories. The first one is the continuous type. That is, a small variation of a parameter may be compensated by the variations of other parameters. If we use a set of optimum parameters as a starting point for the search routine, it might converge to a slightly different

point in the parameter space leaving χ^2 practically unchanged. The second one is the discrete type. Only certain sets of parameters can give the correct angular distributions. This type of parameter ambiguity will be discussed in the following sections.

3-2.1 Vr_0^n Ambiguity

The potentials in Table 2 can be divided into four groups according to the values of Vr_0^2 . The first five potentials have approximately the same Vr_0^2 . They form a group. The groups with deeper wells have more elements than those of the shallower ones.

$V-r_0$ invariance becomes clear if one examines the wavefunctions. All the radial wavefunctions corresponding to the potentials of the same group have the same number of oscillations inside the nucleus. In other words, V and r_0 are allowed to vary in such a way that the number of waves inside the nucleus is kept constant. Since the wavelength λ for a particular partial wave is approximately the same inside the well, we can write

$$\frac{R}{\lambda} = \text{const.}, \quad (3-1)$$

(53)

where $R = r_0 A^{1/3}$. Neglecting the absorption term, Eq. (3-1) is equivalent to

$$R \sqrt{E+V} = \text{const.} \quad (3-2)$$

For deep wells, $V \gg E$, Eq. (3-2) becomes

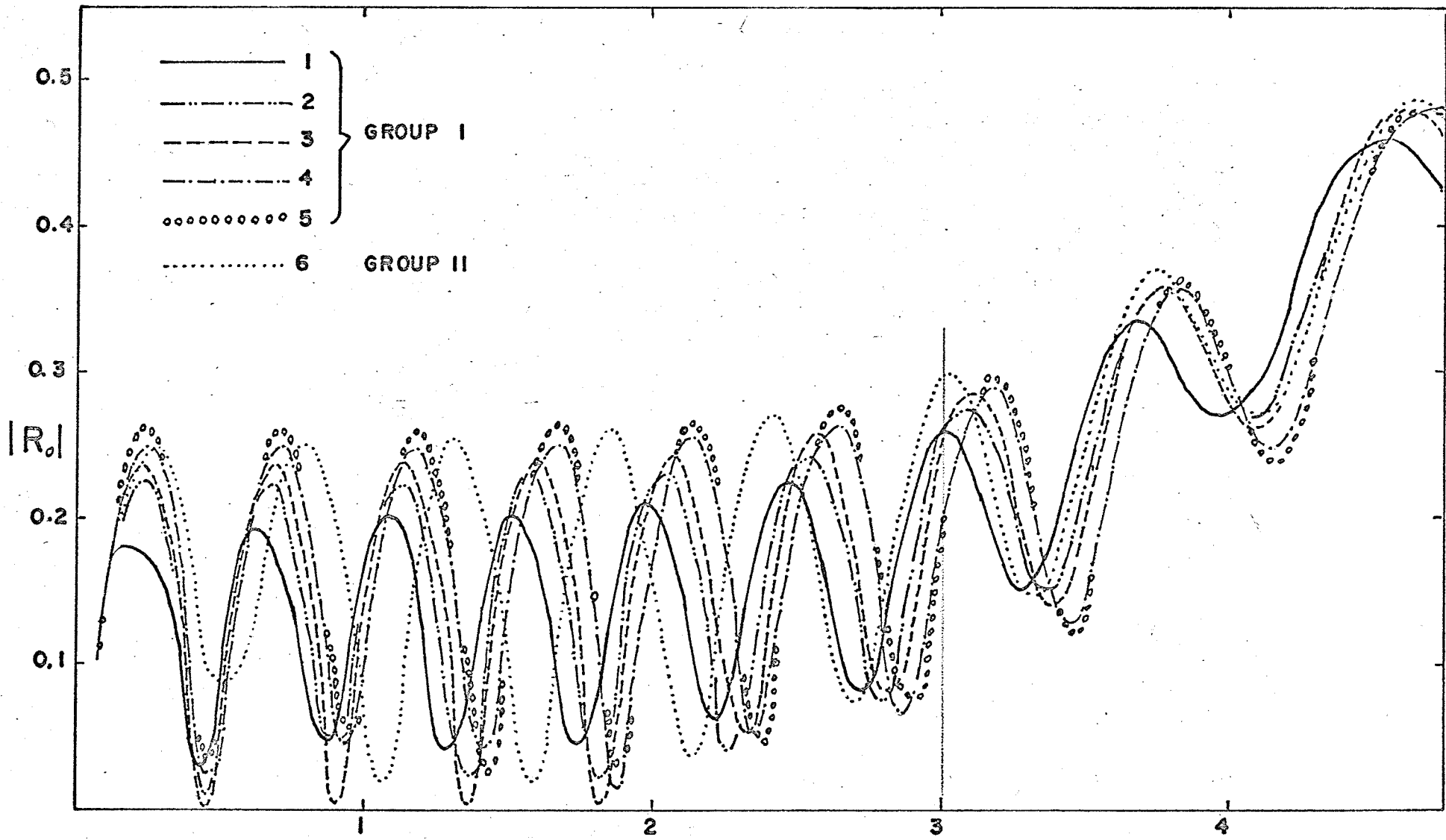
$$R^2 V = \text{const.} \quad (3-3)$$

In this case, n is equal to 2.

Fig. 17

The Amplitudes of the Radial Wavefunctions R_0 .

They all have the same number of oscillations inside the nucleus for the potentials in a group.



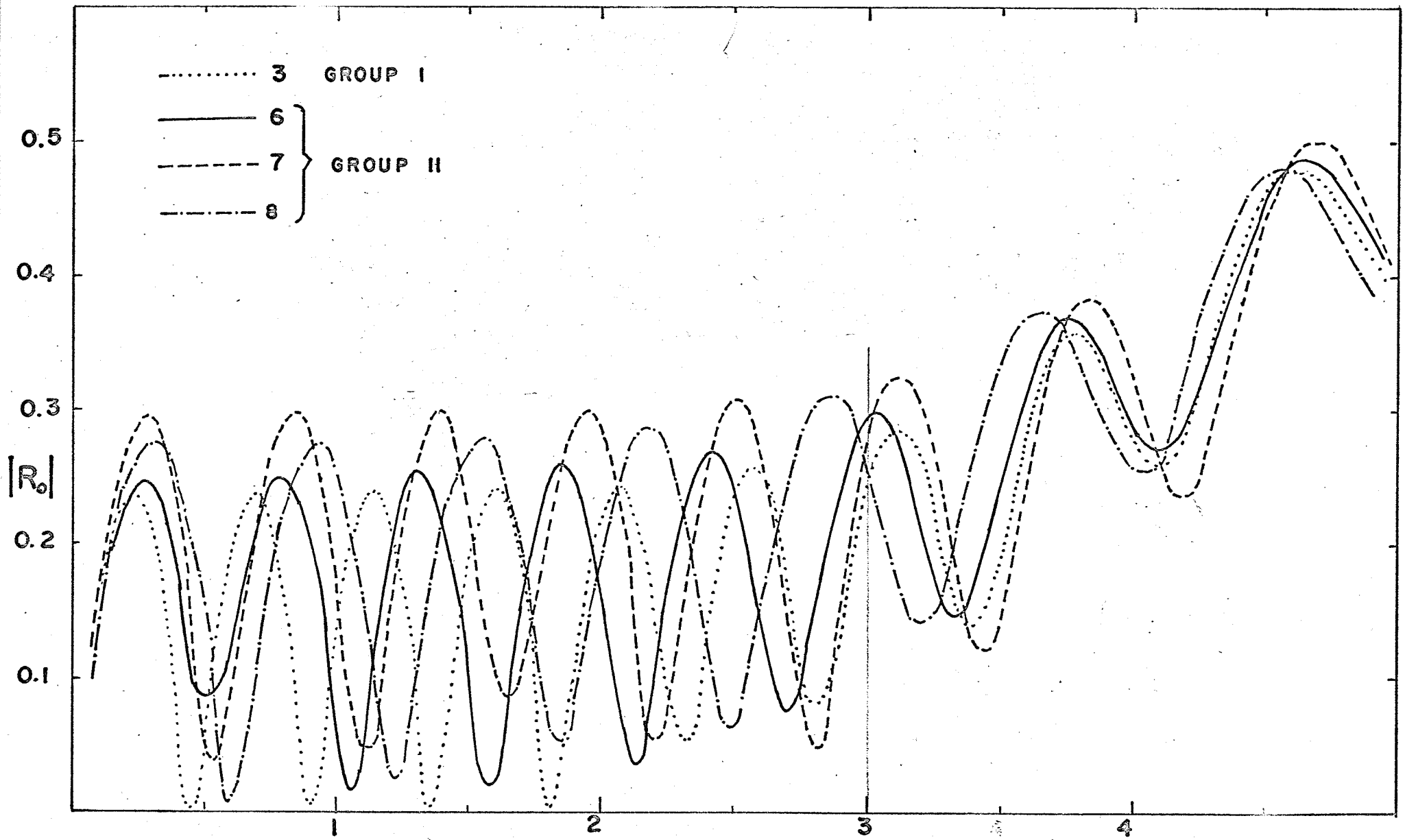
RADIUS IN FERMI

Fig. 17

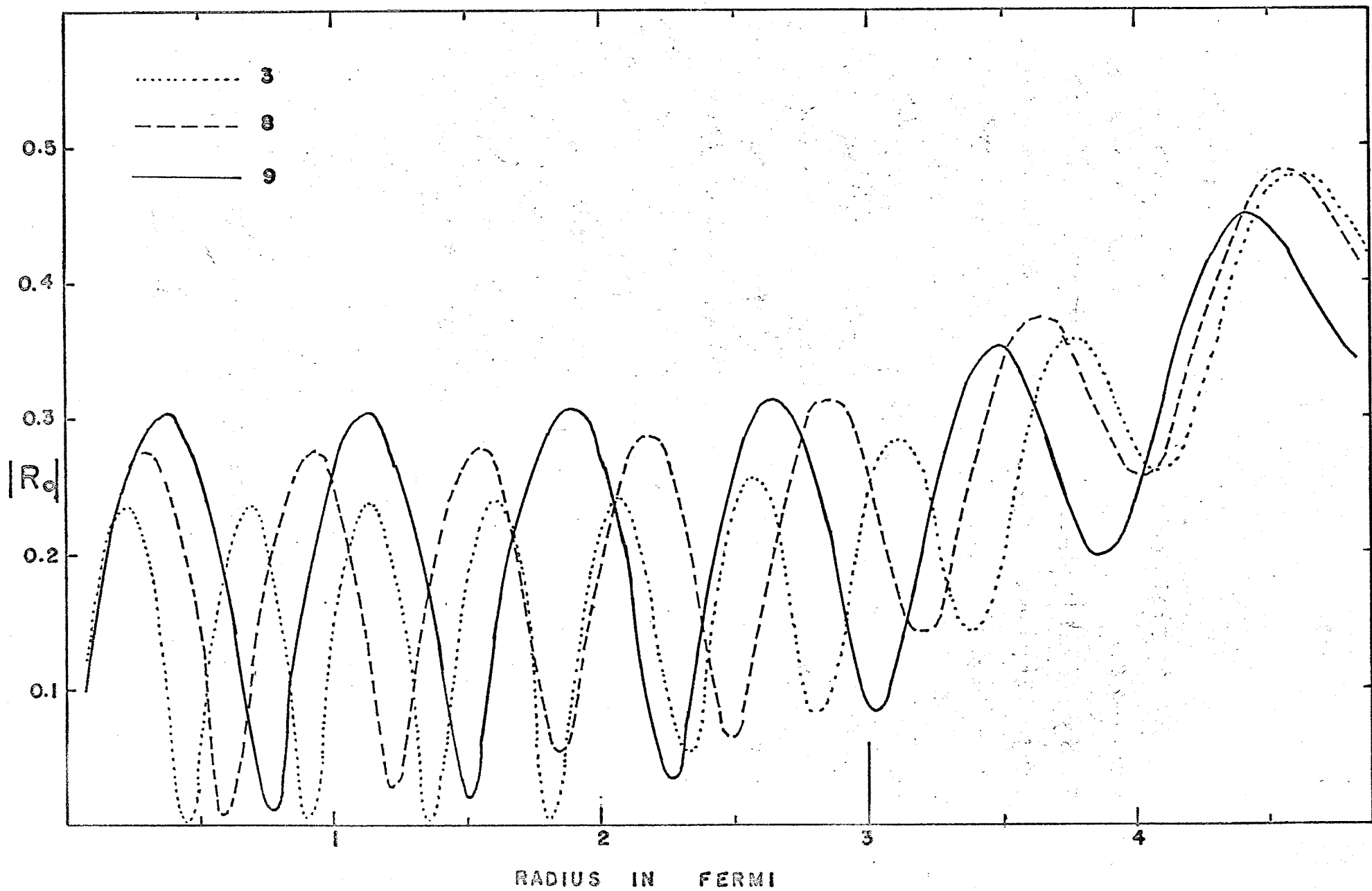
(55)

Fig. 18

The Amplitudes of the Radial Wavefunctions R_0 .



RADIUS IN FERMI
(Fig.18)



(Fig. 19)

3-2.2 Potential Depth Ambiguity

If we examine further the radial wavefunctions of the optimum potentials, it is clear they differ in that the wavefunctions corresponding to the potentials of the same group have one half-wave more inside the nucleus than the next shallower group. The same kind of ambiguity has been found by Drisko et al^{*}) in 1963 when they did the optical model fit to the α -Ni⁵⁸ elastic scattering at 43 Mev. Austern interpreted this type of ambiguity by employing WKB approximation. He expressed scattering matrix elements for each partial wave as the sum of two terms, one due to the absorption in the nuclear surface and the other due to the angular momentum barrier and the absorption in the nuclear interior. From Fig. 14 we can see that low partial waves with $\ell < 13$ are strongly absorbed. The higher partial waves are mainly affected by the nuclear surface, while the lower ones penetrate further into the nuclear interior. For low partial waves the scattering coefficients can be written

$$\eta_{\ell} \equiv e^{2i \delta_{\ell}(r)}, \quad (3-4)$$

*) R. M. Drisko, G. R. Satchler, and R. H. Bassel, Phys. Lett. 5 (1963) 347.

**) N. Austern, Ann Phys. 15 (1961) 299.

where the phases $\delta_\ell(r)$ are related to the potential depths by

$$\delta_\ell(r_\ell) = C_\ell + \int_{r_\ell}^{\infty} \left[\frac{2\mu}{\hbar^2} (E - V_c(r) - V_n(r) - \frac{\ell(\ell+1)}{r^2}) \right]^{1/2} dr. \quad (3-5)$$

C_ℓ is a constant independent of the potential depth and r_ℓ is the classical turning point, i.e., $E = V(r_\ell)$. This type of parameter ambiguity can be understood from Eq. (3-4) and (3-5). If a series of potentials with different depth are such that they generate the phases δ_ℓ which differ by an integral multiple of π , then η_ℓ 's are the same.

This type of parameter ambiguity is not important for elastic scattering since it is determined only by the asymptotic wavefunctions and these are the same for all the potentials in the series. However, the DWBA calculations of cross-sections for nuclear reactions involve the integrations of the wavefunctions throughout space and are clearly sensitive to the number of oscillations of the wavefunctions inside the nuclear interior. It is important in this case to know which potential is physically correct.

3-3 The Surface Region of -0^{16} Optical Potential

Although the optical parameters cannot be determined uniquely by the present analysis, it does define the optical potential as a whole fairly well near the nuclear surface. This is shown in Fig. 1 and 2. All the real parts of the optimum potentials have the same type of surfaces. The imaginary parts also resemble each other near the nuclear surface. These give another evidence that the interactions of α -particle with the target nucleus is more important on the surface, although, as already stated in the previous section, the nuclear volume also influences the angular distributions through the low partial waves.

3-4 Summary and Conclusion

The optical model analysis has become a standard method to find out the nucleon-nucleus potentials. They have been used successfully in the DWBA calculations of nuclear reactions. The present work is to determine the -0^{16} optical potential in an attempt to extend the optical analysis to the interactions involving composite particles. The applicability of this method to the double magic helium nuclei can be expected.

The optical analysis of the α - ^{16}O experimental data yields a set of complex potentials. All of them can reproduce quite well the angular distributions. Which one of these potentials is physically correct cannot be determined by the elastic scattering measurements only. Since the actual calculations of the elastic cross-sections merely use the asymptotic wavefunctions, that is, all the potentials which can reproduce the same wavefunctions outside the nuclear field will have the same angular distributions. However the DWBA calculations involve the integration of the wavefunctions through space. It provides a way of judging the potentials determined by the present analysis.

Two types of parameter ambiguity have been found for the α - ^{16}O optical potentials. The first type is that the optical parameters are allowed to vary, with the quantity Vr_0^2 kept constant. The potentials belonging to this category are listed in groups in Table 2. V - r_0 invariance can be understood by examining the wavefunctions. The amplitudes of the radial wavefunctions for a given l corresponding to the potentials in a group have the same number of half-waves inside the nucleus. The second type is that the

parameters can be adjusted so that they produce one or more integral multiple half-waves inside the nucleus such that the corresponding amplitudes of the wavefunctions far away from the nuclear field are the same. This is the formation of the different groups of potentials on Table 2. Each group has one more half-wave than the next shallower one.

Although the optical potential is not uniquely determined by the present analysis, it defines the phenomenological potential quite well near the surface. This gives an evidence that the interaction of alpha particles with the target nucleus is more important on the nuclear surface.

(62)

Fig. 20

Variation in $\frac{dS}{dR}$ with r_c

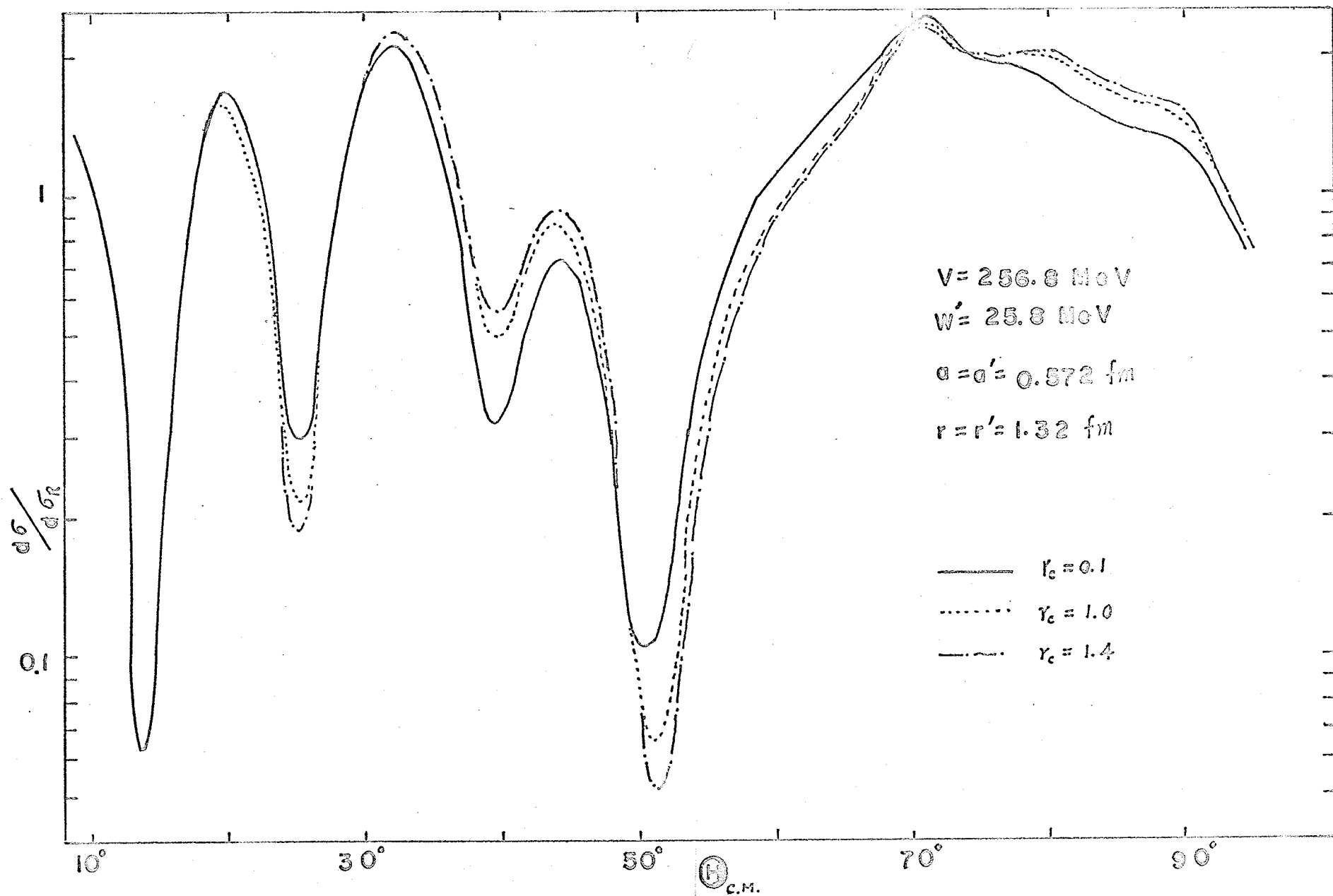


Fig. 20

\oplus c.m.

APPENDIX

C AUTOMATIC SEARCH OF OPTICAL PARAMETERS
C
C UP TO 7 PARAMETERS CAN BE CYCLED AT ONCE.
C INPUT
CARD1. (NNN) NUMBER OF EXPT. POINTS.
CARD2. (SIGMAE THETA DSIGMA) ARE THE EXPT. DATA, ANGLES,
C AND THE ERROR AT EACH EXPERIMENTAL POINT.
CARD3. (R,A,R',A',V,W,W') ARE THE OPTICAL PARAMETERS.
C AFTER ONE RUN THE PROGRAM GOES BACK TO CARD 3.
CARD4. (DR,DA,DR',DA',DV,DW,DW',NC) ARE THE INCREMENTS OF THE OPTICAL
C PARAMETERS, NC IS THE NUMBER OF CYCLES.
C LET W BE ONE OF THE PARAMETERS. IF DW/W IS LESS THAN 0.01,
C CYCLING OF THIS PARAMETER STOPS..
CARD5. (M2,M1,Z,RC,DE,LMAX,E)
C M2 IS THE MASS OF TARGET IN AMU.
C M1 IS THE MASS OF THE BEAM PARTICLE IN AMU.
C Z IS THE PRODUCT OF CHARGES OF TARGET AND BEAM PARTICLE.
C RC*1/3 POWER OF M2 IS THE COULOMB RADIUS.
C DE= INTEGRAL INCREMENT
C LMAX= MAXIMUM VALUE OF ORBITAL ANGULAR MOMENTUM.
C E= ENERGY IN LAB.
C
C WHEN THE DIRECTION OF THE SEARCH IN W CHANGES , DW IS HALVED.
C WHEN W CHANGES IN THE SAME DIRECTION FOR FIVE CONSECUIVE CYCLES,
C DW IS DOUBLED
C
C OPTION
C
C + *****
C DE
C - TYPE OUT ETAMOD, ETAARG DURING THE FIRST CYCLE.
C
C + TYPE OUT DISTRIBUTION EACH CYCLE.
C Z
C - TYPE OUT DISTRIBUTION ON THE LAST CYCLE ONLY.
C
C + PUT VOLUME IMAGINARY PARAMETERS=SURFACE IMAGINARY PARAMETERS.
C LMAX
C - PUT VOLUME IMAGINARY PARAMETERS= REAL PARAMETERS.
C
C + SIGMAT IN MB/SR.
C WE
C - SIGMAT RELATIVE TO RUTHERFORD CROSS SECTION.
C
C + *****
C RC
C - PUT R'=R, A'=A
C
C + INPUT DSIGMA ARE FRACTIONAL ERRORS.
C M1

C - INPUT DSIGMA ARE ACTUAL ERRORS.

```

C.....
  DIMENSION SIGMAT(100),SIGMAE(100),DSIGMA(100),THETA(100),W(7),DW(7
1),ETAMOD(26),ETAARG(26),WT(7),G(7),EXVEC(7),S(7),GB(7),CN(7)
  COMMON SIGMAT,WM2,WM1,WZ,RC,DE,WLMAX,WE,NN,NNN,THETA,
  1ETAMOD,ETAARG,T64,T68,T69
36 FORMAT (4H M2=,F8.4,4X,4H M1=,F8.4,4X,3H Z=,F8.4,4X,3HRC=,F8.4,4X,
  14H DE=,F8.4,4X,6H LMAX=,F8.4,4X,3H E=,F8.4)
37 FORMAT (7F10.4,I4)
38 FORMAT (I4)
  NN=0
  READ (1,38) NNN
43 FORMAT (4(F8.3,F6.2,F6.3))
  READ (1,43) (SIGMAE(I),THETA(I),DSIGMA(I),I=1,NNN)
  WRITE (3,46)
46 FORMAT (1H /4(33H      SIGMA      THETA      DSIGMA ))
  WRITE (3,41) (SIGMAE(I),THETA(I),DSIGMA(I),I=1,NNN)
  8 READ (1,37) (W(I),I=1,7)
  READ (1,37) ((DW(I),I=1,7),NC)
  READ (1,37) WM2,WM1,WZ,RC,DE,WLMAX,WE
  WRITE (3,36) WM2,WM1,WZ,RC,DE,WLMAX,WE
44 FORMAT (4HDR=,F10.4,2X,4H DA=,F10.4,2X,4HDRD=,F10.4,2X,4HDAD=,
  1F10.4,2X,4H DV=,F10.4,2X,4H DW=,F10.4,2X,4HDWD=,F10.4,2X,4H L=,I4
  2,4H NC=,I4)
  T1=DE
  DE=ABS (DE)
  T2=WZ
  WZ=ABS(WZ)
  T69=RC
  RC=ABS(RC)
  T64=WLMAX
  WLMAX=ABS(WLMAX)
  T68=WE
  WE=ABS(WE)
  T3=WM1
  WM1=ABS)WM1*
  IF (NN) 19,19,14
19 IF (T3) 14,14,15
15 DO 16 I=1,NNN
16 DSIGMA(I)=DSIGMA(I)*SIGMAE(I)
14 DO 5 J=1,7
  5 CN(J)=0.
  DO 6 L=1,NC
  WRITE (3,44) ((DW(I),I=1,7),L,NC)
  WRITE (3,39) W(1),W(2),W(3),W(4),W(5),W(6),W(7)
  CALL ELSCAT (W(1),W(2),W(3),W(4),W(5),W(6),W(7))
39 FORMAT (4H R=,F10.4,2X,4H A=,F10.4,2X,4H RD=,F10.4,2X,4H AD=,
  1F10.4,2X,4H V=,F10.4,2X,4H W=,F10.4,2X,4H WD=,F10.4)
41 FORMAT (1H /4(1H ,F12.4,2F10.4))
  CHISQ=0.
  DO 29 I=1,NNN
  CHI=(SIGMAT(I)-SIGMAE(I))/DSIGMA(I)
29 CHISQ=CHI*CHI+CHISQ

```

```

CHISQ=CHISQ/NNN    $\chi^2$ 
IF (T1) 17,18,18
17 WRITE (3,47) ETAMOD
   WRITE (3,47) ETAARG
47 FORMAT (1H / (10F12.4))
   T1=DE
18 WRITE (3,45) CHISQ
   IF (L-NC) 1,12,12
45 FORMAT (15H CHI SQUARED = ,E12.5)
C  CALCULATE THE DERIVATIVES OF CHI-SQUARED
   GNORM=0.0
   N=0
   DO 7 J=1,7
     IF (DW(J)/W(J)-0.01) 7,7,3
3  N=N+1
   WT(N)=ABS(DW(J))
   W(J)=W(J)+WT(N)*0.01
   CALL ELSCAT (W(1),W(2),W(3),W(4),W(5),W(6),W(7))
   W(J)=W(J)-WT(N)*0.01
   G(N)=0.0
   DO 4 I=1,NNN
     CHI=(SIGMAT(I)-SIGMAE(I))/DSIGMA(I)
4  G(N)=G(N)+CHI*CHI
     G(N)=G(N)/NNN
     G(N)=(G(N)-CHISQ)/CHISQ    $\frac{\Delta f}{f}$ 
     GNORM=GNORM+ABS(G(N)/WT(N))
7  CONTINUE
     GNORM=GNORM+0.2
     IF(N)12,12,593
593 IF (T2) 594,594,595
595 WRITE (3,41) (SIGMAT(I),THETA(I),DSIGMA(I),I=1,NNN)
594 DO 541 I=1,N
541 EXVEC(I)=-G(I)/(GNORM*WT(N))
     DO 543 I=1,N
       IF(EXVEC(I))543,543,544
543 S(I)=-1.
       GO TO 545
544 S(I)=1.
545 EXVEC(I)=ABS(EXVEC(I))
546 EXVEC(I)=SQRT(EXVEC(I))
548 EXVEC(I)=S(I)*EXVEC(I)
     IF(L-1)10,10,9
     IF(L-1)10,10,9
9  N=0
     DO 590 J=1,7
       IF (DW(J)/W(J)-0.01) 590,590,25
25  N=N+1
     IF (G(N)/GB(N)) 585,585,591
585 DW(J)=DW(J)/2.
     CN(N)=0.
     GO TO 590
591 CN(N)=CN(N)+1.
     IF (3.5-CN(N)) 592,592,590

```

$\sum_n \frac{1}{f} \frac{\partial f}{\partial x_n}$

$\text{sign of } -\frac{1}{f} \frac{\partial f}{\partial x_n}$

$\left(\text{sign of } -\frac{1}{f} \frac{\partial f}{\partial x_n} \right) \sqrt{\frac{\frac{1}{f} \frac{\partial f}{\partial x_n}}{\sum_n \frac{1}{f} \frac{\partial f}{\partial x_n}}}$

```

592 DW(J)=DW(J)*2.
      CN(N)=0.
590 CONTINUE
10  N=0
      DO 6 J=1,7
          IF (DW(J)/W(J)-0.01) 6,6,11
11  N=N+1
          W(J)=W(J)+EXVEC(N)*WT(N)
          GB(N)=G(N)
6   CONTINUE
12  WRITE (3,41) (SIGMAT(I),THETA(I),DSIGMA(I),I=1,NNN)
      WRITE (3,48)
48  FORMAT (1H1)
      GO TO 8
      END

```

```

SUBROUTINE ELSCAT (WR,WA,WRO,WAD,WV,WV,WWD)
14  DIMENSION P(99),B(111),A(64),A1(8),V(4),F(26,4),H(1003),U(1003),
      1S(1002),E(32,6),Q(32,3),PV(3),H4(20),C1(26),S1(26),SG(27),PI(99),
      2C4(3),SIGMAT(100),THETA(100),ETAMOD(26),ETAARG(26)
      COMMON SIGMAT,WM2,WM1,WZ,RC,DE,WLMAX,WE,NN,NNN,THEIA,
      1ETAMOD,ETAARG,T64,T68,T69
      IF (NR) 7,7,10
7   NN=1
      DO 6 I=1,NNN
6   B(I)=COS(THETA(I)*0.017453)  cos θ
      TU=EXP(ALOG(WM2)/3.)  A1/3
      N1=INT(WLMAX+1.)
      H2=WM2/(WM2+WM1)
      W2=WM1*H2  μ
      H2=WE*H2  Ecm = Elab * M2 / (M1+M2)
      W1=.04784614*W2
      H2=W1*H2  k2 = 2μEcm/ħ2
      H1=SQRT(H2)  ħ
      Z=WZ*W1*.7199495/H1  γ
      Z2=Z*Z
      DO 17 I=1,17,16
          A(I)=1.
17  A(I+32)=0.
          A(64)=0.
          T1=1.
          T2=2.
          T3=0.
      DO 19 I=1,15
          T5=T1*Z/T2  Am = (2m+1) / (2(m+1)) γ

```

```

T4=-T3*(T3+1.)+Z2
T7=(2.+T4)/T2
T6=T4/T2   $B_m^0$ 
A(I+1)=T5*A(I) - T6*A(I+32)   $S_{m+1,0} = A_m S_{m,0} - B_m^0 t_{m,0}$ 
A(I+17)=T5*A(I+16)-T7*A(I+48)   $S_{m+1,1} = A_m S_{m,1} - B_m^1 t_{m,1}$ 
A(I+33)=T6*A(I)+T5*A(I+32)
A(I+49)=T7*A(I+16)+T5*A(I+48)
T3=T3+1.
T1=T1+2.
19 T2=T2+2.
TM=20.
DO 22 I=32,64,32
IF(A(I))20,22,20
20 T1=(10.**((6.+43429448*ALOG(ABS(A(I))))/15.))/H1  radius where  $S_m \approx 10$ 
IF(T1-TM)22,22,21
21 TM=T1
22 CONTINUE
500 M1=INT(TM/DE)
IF(M1-1000)24,24,23  } number of radial increments.
23 M1=1000
24 T1=FLOAT(M1)
M2=M1+2
M7=M1+1
D1=TM/T1  radial increment  $\delta$ 
D2=D1*D1
DTT=D2/12.
DT=2.*D1
DT2=2.*D2
DT3=-DT2/12.
W1=D2*W1/12.   $\frac{2M}{4^2} \frac{\delta^2}{12}$ 
H2=1.+DTT*H2
HZ=DT3*H1*Z
T1=Z2+16.
SG(1)=-Z+Z*(ALOG(T1))/2.+3.5*ATAN(Z/4.)-ATAN(Z)-
1ATAN(Z/2.)-ATAN(Z/3.)-Z*(1.+(Z2-48.)/(30.*T1*T1)+
2(Z2*Z2-160.*Z2+1280.)/(105.*T1*T1*T1*T1))/(12.*T1)  }  $\sigma$ 
T1=0.
DO 27 I=1,N1
T1=T1+1.
C1(I)=COS(SG(I))  }  $e^{i\sigma_{I-1}}$ 
S1(I)=SIN(SG(I))
27 SG(I+1)=SG(I) + ATAN(Z/T1)   $\sigma_I = \sigma_{I-1} + \tan^{-1} \frac{Z}{I}$   } calculate Coulomb phase shifts.

```

```

T1=TM+DT
DO 107 I=1,2
T1=T1-D1
T2=T1*H1  $\rho = kY$ 
T3=T2-Z *ALOG(2.*T2)+SG(1)  $\theta_0 = KY - \gamma \ln 2\rho + \sigma_0$ 
T9=T3-1.5707963+ATAN(Z)  $\theta_1 = \theta_0 - \frac{\pi}{2} + \sigma_0 + \tan^{-1}\left(\frac{\gamma}{1}\right)$ 
T4=T2
DO 28 K=1,4
T4=T4*T4
28 V(K)=0.
DO 29 K=1,16
V(1)=(V(1)+A(K)) *T2  $\rho^{16} S_0 = \sum_{m=1}^{16} S_{m,0} (KY)^{16-m}$ 
V(2)=(V(2)+A(K+16))*T2
V(3)=(V(3)+A(K+32))*T2
29 V(4)=(V(4)+A(K+48))*T2
DO 30 K=1,4
30 V(K)=V(K)/T4
T5=COS(T3)  $\left. \begin{array}{l} T5=COS(T3) \\ T6=SIN(T3) \end{array} \right\} e^{-i\theta_0}$ 
T6=SIN(T3)
T7=COS(T9)  $\left. \begin{array}{l} T7=COS(T9) \\ T8=SIN(T9) \end{array} \right\} e^{-i\theta_1}$ 
T8=SIN(T9)
S(1)=V(1)*T5-V(3)*T6  $G_0$ 
U(1)=V(2)*T7-V(4)*T8  $G_1$ 
H(1)=H2+HZ/T1
107 C4(1)=H(1)+DT3/(T1*T1)
T1=T1-D1
H(3)=H2+HZ/T1
C4(3)=H(3)+DT3/(T1*T1)
S(3)=((12.-10.*H(2))*S(2)-H(1)*S(1))/H(3)
108 U(3)=((12.-10.*C4(2))*U(2)-C4(1)*U(1))/C4(3)
F(1,3)=S(3)  $G_0(\gamma_{max} - \delta)$ 
F(1,4)=S(2)  $G_0(\gamma_{max})$ 
F(2,3)=U(3)  $G_1(\gamma_{max} - \delta)$ 
F(2,4)=U(2)  $G_1(\gamma_{max})$ 
DO 32 I=1,2
T2=T1*H1
T10=1./T2
T1=T1+D1
T7=0.
N8=0
N6=INT((T2/1.4142)*SQRT(25.-2.*Z *T10+10.*SQRT((Z *T10-.5)
1**2+6.)))
IF(N6-N1-8)88,89,89
88 N6=N1+3  $\gamma_{max}$  for Coulomb wave functions
89 T6=FLOAT(N6)
MW=0
N7=N6+1
H(N7+1)=0.
T5=T7  $\text{--- calculated } F_1/F_0$ 
H(N7)=1.0E-70
S(N7)=SQRT(Z2 +(T6+1.)**2)/(T6+1.)
DO 100 K=1,N6
M=N7-K
IF(ABS(H(M+1))-1.0E+34)700,701,701

```

```

701 H(M+1)=H(M+1)*1.0E-30 } overflow prevention
    H(M+2)=H(M+2)*1.0E-30
    MW=M

```

```

700 IF (N8-M)104,106,105
104 S(M)=SQRT (Z2 +T6*T6)/T6  $\sqrt{\gamma^2 + l^2} / l$ 
    U(M)=(2.*T6+1.)*(Z / (T6*(T6+1.))+T10)  $(2l+1) \left( \frac{\gamma}{2(l+1)} + \frac{1}{\rho} \right)$ 
    T6=T6-1.

```

```

106 H(M)=(U(M)*H(M+1)-S(M+1)*H(M+2))/S(M) recursion formula for  $F_2$  &  $G_2$ 
100 CONTINUE

```

```

N8=N6
N6=N6+10
IF (N6-1000)31,01,1016

```

```

31 T7=H(2)/H(1)
IF (ABS((T5-T7)/T7)-0.0001)101,101,89
101 T5=1./(S(1)*(H(1)*F(2,I+2)-H(2)*F(1,I+2)))
    F(1,I)=T5*H(1)
    F(2,I)=T5*H(2)
    DO 32 K=3,N1
        IF (MW-1)703,704,704

```

normalization factor c

$$c = \frac{1}{\sqrt{2} (F_2 G_1 - F_1 G_2)}$$

```

704 IF (K-MW)703,750,705
750 H(K-2)=H(K-2)*T5
    H(K-1)=H(K-1)*T5
705 H(K)=(U(K-2)*H(K-1)-S(K-2)*H(K-2))/S(K-1)
    F(K,I)=H(K)
    GO TO 706

```

} Normalize F_2 & G_2

```

703 F(K,I)=T5*H(K)
706 F(K,I+2)=(U(K-2)*F(K-1,I+2)-S(K-2)*F(K-2,I+2))/S(K-1)
32 CONTINUE

```

```

10 IF (T69) 11,12,12
11 WRD=WR

```

```

WAD=WA
12 H4(8)=WRD* $TU$   $R' = \gamma_0 A^{1/3}$ 
    H4(12)=EXP(D1/WAD)  $e^{s/a}$ 
    H4(16)=1./EXP(H4(8)/WAD)  $e^{-\gamma_0 A^{1/3}/a}$ 
    H4(4)=WR* $TU$   $R = \gamma_0 A^{1/3}$ 
    T1=(1.5*HZ)/(RC* $TU$ )
    H22=H2+T1  $1 + \frac{s^2 \gamma^2}{12 \frac{\gamma^2}{a^2}} \left( E - \frac{3 Z Z' e^2}{2 R_c} \right)$ 
    HZZ=-T1/(3.*RC*RC* $TU$ )
    A1(2)=EXP(D1/WA)  $e^{s/a}$ 
    A1(8)=1./EXP(H4(4)/WA)

```

```

DO 59 I=1,N1
UNDER=1.
Q(I,1)=0.
Q(I,2)=0.
DO 59 J=1,4,3
E(I,J)=0.
E(I,J+2)=0.
59 E(I,J+1)=(DE**I)*DE*UNDER
PV(1)=0.
PV(2)=0.
H4(18)=4.*WWD*W1

```

2nd boundary condition

$$E(I,1) = 0, \quad E(I,2) = \delta^{2+1}, \quad E(I,3) = 0$$

$$\gamma = -\delta, \quad \gamma = 0, \quad \gamma = +\delta$$

```

T1=0.
DO 67 J=1,M1
T1=T1+D1
T2=T1*T1 (r-R)/a
A1(8)=A1(8)*A1(2) e
IF (A1(8)-1.0E+30) 2010,2009,2009
2009 A1(8)=1.0E+30
2010 T7=W1/(1.+A1(8))
H4(16)=H4(16)*H4(12)
IF (H4(16)-1.0E+30) 2012,2011,2011
2011 H4(16)=1.0E+30
2012 IF (T64) 127,62,62
62 T7T7=T7
GO TO 209

```

imaginary volume (geometrical) parameters = real parameters

```

127 T7T7=W1/(1.+H4(16))
209 IF (T1-RC*TU)60,61,61
60 R=H22+HZZ*T2+WV*T7  $1 + \frac{\delta^2 \mu}{12 \frac{\mu}{\lambda^2}} \left( \epsilon_{cm} - \frac{3ZZ'e^2}{2 R_c} + \frac{ZZ'e^2}{R_c^3} r^2 + \frac{V}{1+e \frac{(r-R)}{a}} \right)$  inside the charged sphere
GO TO 126
61 R=H2+HZ/T1+WV*T7  $1 + \frac{\delta^2 \mu}{12 \frac{\mu}{\lambda^2}} \left( \epsilon_{cm} - \frac{ZZ'e^2}{F} + \frac{V}{1+e \frac{(r-R)}{a}} \right)$  outside the sphere.
126 T3=H4(16)/((1.+H4(16))* (1.+H4(16)))
PV(3)=H4(18)*T8+WW*T7T7

```

surface absorption

```

212 T3=0.
T6=0.
125 DO 68 I=1,N1 I = l+1 (partial waves)
T6=T6+DT3
Q(I,3)=R+T3/T2
T8=12.-10.*Q(I,2)
T9=10.*PV(2)
T10=Q(I,3)*Q(I,3) + PV(3)*PV(3)
T4=T8*E(I,2)-Q(I,1)*E(I,1)+T9*E(I,5)+PV(1)*E(I,4)
T5=T8*E(I,5)-Q(I,1)*E(I,4)-T9*E(I,2)-PV(1)*E(I,1)
E(I,3)=(Q(I,3)*T4+PV(3)*T5)/T10
E(I,6)=(Q(I,3)*T5-PV(3)*T4)/T10
63 T3=T3+T6
PV(1)=PV(2)
PV(2)=PV(3)
DO 67 I=1,N1
Q(I,1)=Q(I,2)
Q(I,2)=Q(I,3)
DO 67 K=1,5
E(I,K)=E(I,K+1)
67 CONTINUE
SIGMAR=0.
AI=0.
DO 68 I=1,N1
T8=E(I,2)*E(I,2) + E(I,5)*E(I,5)

```

$$E(I,1) = Re \mathcal{F}_l^{(1)}(r-2\delta)$$

$$E(I,2) = Re \mathcal{F}_l^{(2)}(r-\delta)$$

$$E(I,3) = Re \mathcal{F}_l^{(3)}(r)$$

$$E(I,4) = Im \mathcal{F}_l^{(4)}(r-2\delta)$$

$$E(I,5) = Im \mathcal{F}_l^{(5)}(r-\delta)$$

$$E(I,6) = Im \mathcal{F}_l^{(6)}(r)$$

```

T1=(E(I,1)*E(I,2) + E(I,4)*E(I,5))/T8 > Re & Im of  $\frac{F_1(r-s)}{F_2(r)}$ 
T2=(E(I,4)*E(I,2) - E(I,1)*E(I,5))/T8
T5=F(I,1) - F(I,2)*T1
T6=F(I,2)*T2
T3=T5 - F(I,4)*T2
T4=T6 + F(I,3) - F(I,4)*T1
T7=T3*T3 + T4*T4
T1=(T3*T5 + T4*T6)/T7 >  $\beta_1$ 
T2=(T4*T5 - T3*T6)/T7
T3=C1(I)*C1(I)*2. - 1.
T4=C1(I)*S1(I)*2.
AI=AI+1.
DO 1015 K=1,NNN
SN=(1.-B(K))*0.5  $\sin^2 \theta/2$ 
IF (I-2)1009,1012,1010
1009 P(K)=1.  $P_0(\omega_0)$ 
C2=Z *ALOG(SN)
S2=SIN(C2) >  $e^{2iZ \ln(\sin \theta/2)}$ 
C2=COS(C2)
U(K+53)=-((T3*C2+T4*S2)*Z/(2.*H1*SN)) >  $f_c(\omega)$ 
U(K+154)=((T3*S2-T4*C2)*Z/(2.*H1*SN))
GO TO 1013
1012 P(K)=B(K)
PT(K)=1. }  $P_1(\omega_0)$ 
GO TO 1013
1010 T6=P(K)
P(K)=((2.*AI-3.)*B(K)*T6-(AI-2.)*PT(K))/(AI-1.) recursion formula for  $P_2(\omega_0)$ 
PT(K)=T6
1013 U(K+53)=U(K+53)-(2.*AI-1.)*P(K)*(T1*T4+T2*T3)/H1 } scattering amplitude
U(K+154)=U(K+154)+(2.*AI-1.)*P(K)*(T1*T3-T2*T4)/H1
1015 CONTINUE
ETAMOD(I)=SQRT((2.*T1-1.)*(2.*T1-1.)+4.*T2*T2)  $|\eta_R|$ 
ETAARG(I)=ATAN(T2/(T1-0.5))*57.2958  $\arg \eta_R$ 
SIGMAR=SIGMAR+(2.*AI-1.)*(1.-ETAMOD(I)*ETAARG(I))  $\sigma_R$ 
68 CONTINUE
SIGMAR=31.415926*SIGMAR/(H1*H1)
DO 1014 K=1,NNN
1014 SIGMAT(K)=(U(K+53)*U(K+53)+U(K+154)*U(K+154))*10.
IF (T68) 1017,1016,1016
1017 DO 1018 K=1,NNN
SN=(1.-B(K))
O=-Z/(H1*SN)
1018 SIGMAT(K)=SIGMAT(K)/(10.*O*O)  $5/10R$ 
1016 RETURN
END

```

REFERENCES

- (1) Fernbach, Serber, and Taylor, Phys. Rev. 75 (1949) 1352.
- (2) R. E. LeLevier and D. S. Saxon, Phys. Rev. 87 (1952) 40.
- (3) H. Feshbach, C. E. Porter, and V. F. Weisskopf, Phys. Rev. 96 (1954) 448.
- (4) P. E. Nemirovskii, 'Contemporary Models of the Atomic Nuclei', Pergamon Press 1963.
- (5) H. Feshbach, Annual Review of Nucl. Sci., 1958.
- (6) Proceedings of the 3rd Conference on "Reactions between Complex Nuclei".
- (7) Private communication between Dr. B. Hird and Smith.
- (8) T. Y. Li, Ph.D. Thesis, University of Manitoba, 1967.
- (9) N. F. Mott and H. S. W. Massey, 'The Theory of Atomic Collisions', Oxford Clarendon Press, 1965.
- (10) P. B. Jones, 'The Optical Model in Nuclear and Particle Physics', John Wiley & Sons, 1963.
- (11) P. E. Hodgson, 'The Optical Model of Elastic Scattering', Oxford Clarendon Press, 1963.
- (12) Proc. Intern. Conf. Nuclear Optical Model, Florida Univ. Studies, 1959.
- (13) Humblet and Rosenfeld, Nucl. Phys. 26 (1961) 529.

- (14) R. N. Glover and A. D. W. Jones, Nucl. Phys. 81(1966)268.
- (15) J. K. Dickens and F. G. Perey, Phys. Rev. 138 (1965)B1080.
- (16) L. McFadden and G. R. Satchler, Nucl. Phys. 84 (1966) 177.
- (17) J. R. Rook, Nucl. Phys. 61 (1965) 219.
- (18) G. R. Satchler, Nucl. Phys. 70 (1965) 177.
- (19) R. G. Newton, Journal of Math. Phys., 1 (1960) 319.